UiT
THE ARCTIC UNIVERSITY OF NORWAY

Faculty of Science and Technology

Department of Geology

High-resolution study of selected Dansgaard-Oeschger events and Heinrich event 4 42,189–33,393 cal. years BP

Gravity core JM11-FI-15GC from Fugløy Ridge, northeastern Faeroe Islands Margin

—

Björg Jónsdóttir

Master thesis in Geology (GEO-3900)
May 2015

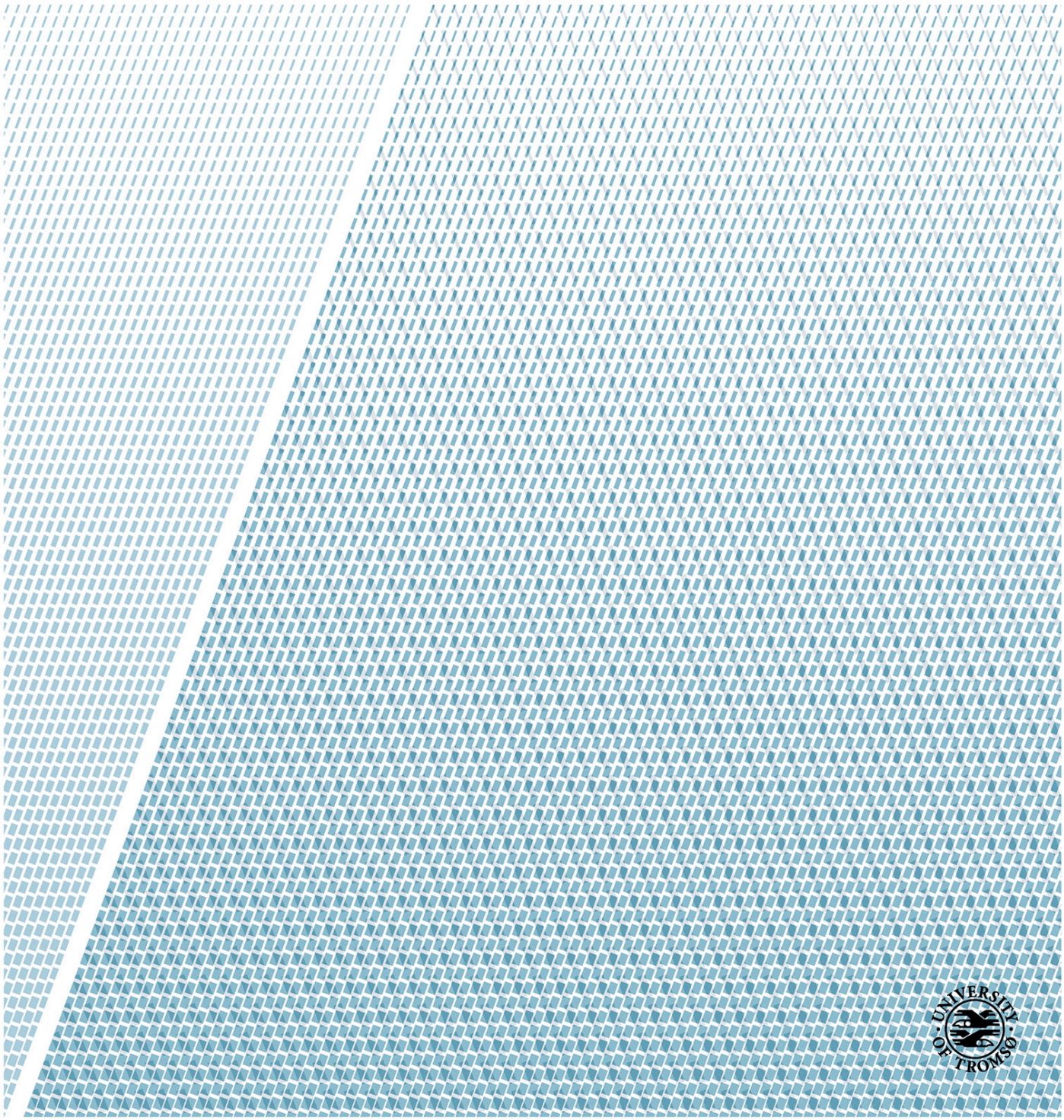

Abstract

The focus of this thesis was selected Dansgaard-Oeschger (D-O) events and Heinrich event 4 (H4). A gravity core, JM11-FI-15GC, from Fugløy Ridge was used for the investigation. The location of the core site is important due the fact that the Faeroe-Shetland Channel is a key area in understanding the changes in circulation during the last glacial period. In total there were eighteen D-O climatic events found within the investigated core. Only part of core JM11-FI-15 GC was used, which is dated to between 42,189 – 33,393 cal. years BP. It is a short interval, comprising a total of four D-O climatic events, which were studied in high-resolution. The events were correlated to the NGRIP ice-core using interstadials and tephra layer FMAZ-III as tie points. The largest D-O event was used as a template, for smaller events, when the data was interpreted. The D-O event was further subdivided into three intervals based on oxygen isotopes, magnetic susceptibility, concentration of planktic foraminifera and ice rafted detritus.

Interstadial intervals had similar circulation as today, with formation of North Atlantic Deep water (NADW). These intervals started abruptly after the colder stadials. Transitional cooling intervals were characterized by reduction in the formation of NADW, with increasing concentration of ice rafted detritus. There was indication that the environment was unstable. During Heinrich event 4 the formation of NADW was either greatly reduced or had stopped. There was high concentration of IRD and increased melt water from icebergs as indicated by low $\delta^{18}O$ values. High concentration of the benthic foraminiferal species *C. neoteretis* indicated the presence of the Atlantic Intermediate water. Fragmentation of foraminiferal tests was used track changes in dissolution. There was low dissolution during the stadials, which was likely caused by low organic productivity. The dissolution obscured the data, indicating the stadials were characterized by warmer surface water then interstadials.

Table of Contents

List of Figures

List of Tables

Acknowledgements

I would first and foremost want to thank my supervisor Tine L. Rasmussen. It was privilege to have her as my supervisor. She was very helpful throughout the whole process, and always greeted me with a smile on her face if I had any questions. Also, the wonderful laboratory staff, who were always helpful if I had some questions or if I needed little help.

I want to thank the Centre for Arctic Gas Hydrate, Environment and Climate (CAGE) for financial support regarding radiocarbon dating and isotope analyses.

The ships captain and the crew on board R/V Helmer Hansen (former R/V Jan Mayen), who participated in the scientific cruise from 26. April - 11. May 2011. And everyone who helped with handling of gravity core JM11-FI-15GC.

Mohamed Ezat and Ulrike Hoff for the GEOTEK data.

My family and friends from back home have been very supportive my whole time in Tromsø. If it had not been for their support I would not be here. I would especially want to thank my oldest brother for his passion, when I was asking for help with computer problems and programs. I also need to thank my office-buddy and friend Erna Ósk Arnardóttir. My boyfriend Jóhannes M. Jóhannesson, who has been very supportive through this whole process, especially during the last few days. And to all the great people I got to know through my stay here. You guys rock!

Björg Jónsdóttir

Tromsø 15.05.2015

1 Introduction

1.1 Objectives

The main objective of this thesis is to study selected Dansgaard-Oeschger events and Heinrich event 4 in high-resolution, to gain better insight to the nature and course of the event and to obtain new information from previous studies. The chosen area is a key area for reconstruction of the past oceanographic changes that occurred during the abrupt Dansgaard-Oeschger events. The core is from the northwestern part of the Faeroe-Shetland Channel, which is an important gateway of inflow of Atlantic surface waters from the south and outflow of deep waters generated by convection in Nordic Seas. The gravity core JM11-FI-15GC was used to reconstruct:

- Bottom currents
- Changes in stable isotopes related to climate and water mass properties
- Changes in surface water and formation of bottom waters
- Dissolution events
- Melting of icebergs

1.2 Study area

The areas in the vicinity of the Faeroe Islands have been proven to be important areas for studying climate change (e.g. Rasmussen et al., 1996a;b; Kissel et al., 1999; Rasmussen and Thomsen, 2004). The oceanic circulations around the islands have not always been the same and this change is well documented in the marine sediments around the islands. The investigated core was taken from a location in the Faeroe-Shetland Channel, which is a key area for studying changes in the circulation of the North Atlantic and Norwegian-Greenland Seas (Rasmussen et al., 1996a). The Faeroe-Shetland Channel is part of the Greenland-Scotland Ridge, which separates the Nordic Seas and the Arctic Ocean from the Atlantic Ocean (Blindheim, 1990; Hansen et al., 2008). The Faeroe-Shetland Channel divides the Scottish continental shelf from the Faeroese plateau (Turrell et al., 1999). Fugløy Ridge (see Figure 1) is located northeast of the Faeroe Islands. The ridge is thought to have formed in the Oligocene and Middle Miocene epochs through compression that caused uplift and folding (Sørensen, 2003).

1.3 Oceanography

1.3.1 Circulation

In the present day the warm and saline Atlantic Surface water flows to the north through the Faeroe-Shetland Channel and into the Norwegian Sea (Hansen and Østerhus, 2000; Hansen et al., 2008). The Atlantic water also flows through the Denmark Strait and across the Iceland-Faeroe Ridge, into the area north of the Greenland-Scotland Ridge (Hansen et al., 2008). This inflow of Atlantic water keeps the sea temperature around the Faeroe Islands at approximately 8 °C (Rasmussen et al., 2002b; Hansen and Østerhus, 2000; Hansen et al., 2008).

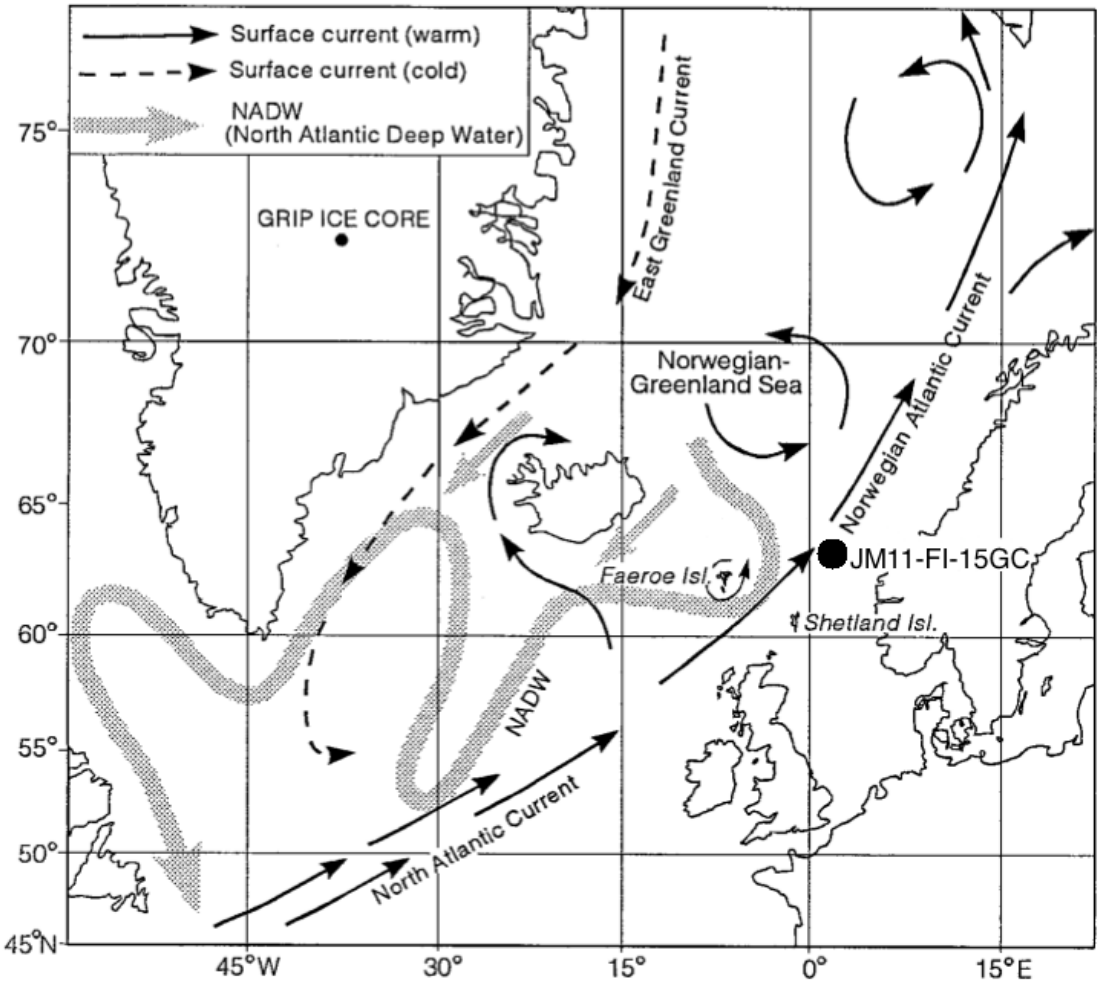

Figure 1 This is a simple model of the formation of the bottom overflow waters. When the water cools and becomes denser it sinks, and drags in warmer water from the south. The figure volume transport of water masses is in Sv (Sverdrup), 1 Sv is 10^6 m^3s^{-1} (figure from Hansen et al., 2008).

As this water mass becomes colder, it becomes denser and sinks in the Norwegian-Greenland Sea (Hansen and Østerhus, 2000). The heat from the water mass

is lost by evaporation to the atmosphere (Gordon, 1986), this helps to maintain the mild climate in northern Europe (Brocker, 1991). This processes forms the North Atlantic Deep Water or NADW. When the denser surface water sinks, more water is drawn in from the south, creating the thermohaline circulation (Gordon, 1986).

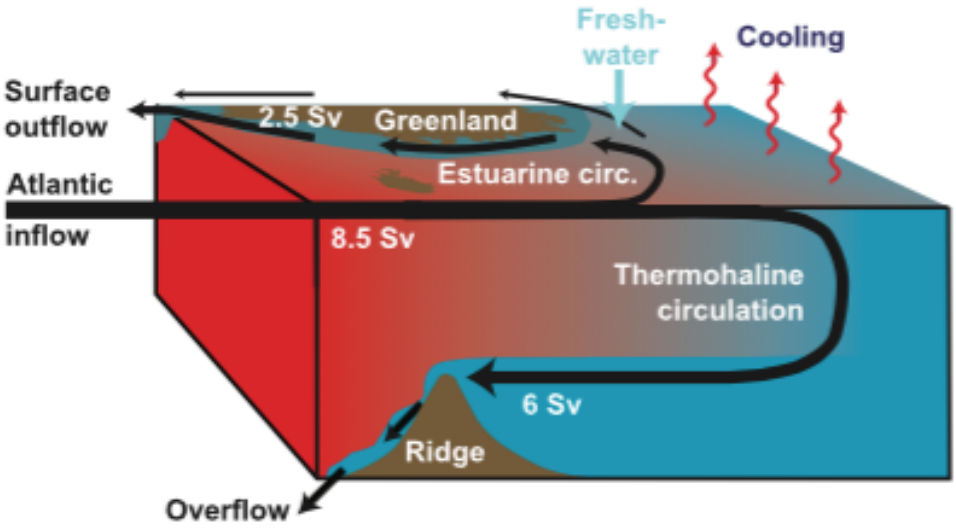

Figure 2 This is a simple model of the formation of the bottom overflow waters. When the water becomes denser it sinks, and drags in warmer water from the south in. On the figure there is Sv, which is abbreviation for Sverdrup. This unit is a measurement of volume transported or 1 Sv is 10^6 m^3s^{-1} (figure from Hansen et al., 2008).

The deep water formed flows through the Denmark Strait, over the Iceland-Scotland Ridge and through the Faeroe-Shetland Channel. The bottom temperature in the Faeroe-Shetland Channel is between -1.0 and -0.5°C (Hansen and Østerhus, 2000).

1.3.2 Water masses

In the Faeroe-Shetland Channel there are five different water masses (Turrell et al., 1999), and the water column is very stratified. The surface waters are of Atlantic origin, which are above the colder and less saline waters from the Norwegian Sea (Borenäs and Lundberg, 2004). There are two distinct surface water masses; the North Atlantic Water (NAW) and the Modified North Atlantic Water (MNAW). The NAW (T > 8 °C) is warmer than the MNAW (-6.5 °C < T <8 °C), and the MNAW is confined to the Scottish slope (Turrell et al., 1999). These surface water masses have different sources, the former is carried by the Continental Slope Current but the latter is derived from an oceanic source (Figure 3) (Hansen et al., 2008).

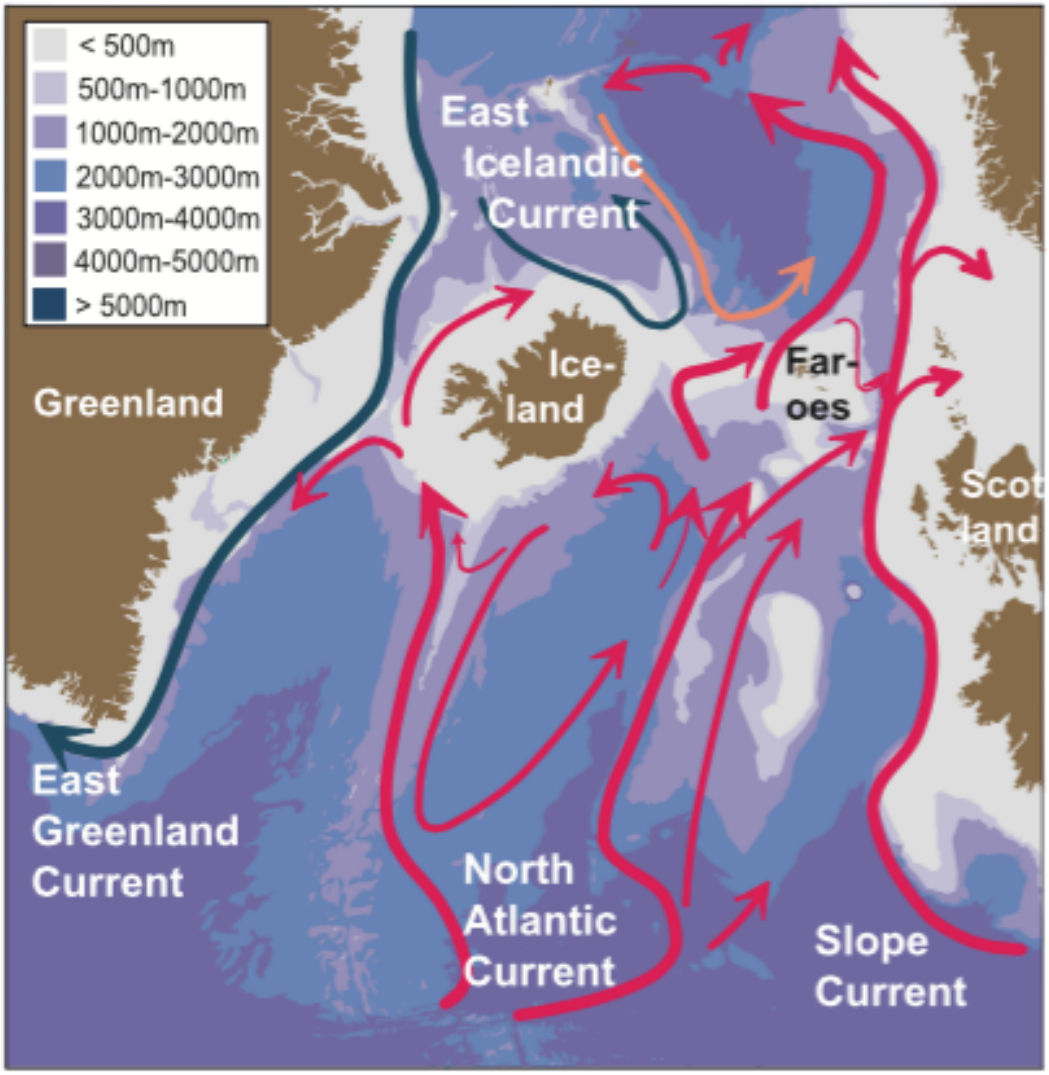

Figure 3 The red arrows show the circulation of the warm North Atlantic Current. The blue arrows indicate colder surface waters (Hansen et al., 2008).

Beneath the surface water masses lies the Arctic Intermediate Water (AIW) with typical potential temperature 2 °C < T < 3 °C (Hansen and Østerhus, 2000). Its origin is north of the Iceland-Faeroe Ridge (Meincke, 1977). The second intermediate water is the Norwegian Sea Arctic Intermediate Water (NSIAW) with typical potential temperature of -0.5 °C < T < 0.5 °C. This water mass is less saline than ambient water masses as seen in Figure 4 (Turrell et al., 1999). The origin of the NSIAW is most likely in the Greenland and Iceland Seas (Blindheim, 1990).

The bottom water found in the Faeroe Shetland Channel is the Faeroe Shetland Bottom Water (FSCBW, formerly known as the Norwegian Sea Deep Water (NSDW)) with T < - 0.5 °C and salinity of 34.90 – 34.92. This water mass is found beneath 800 m

water depth. The bottom water is a mixture of intermediate and deep-water masses (Turrell et al., 1999).

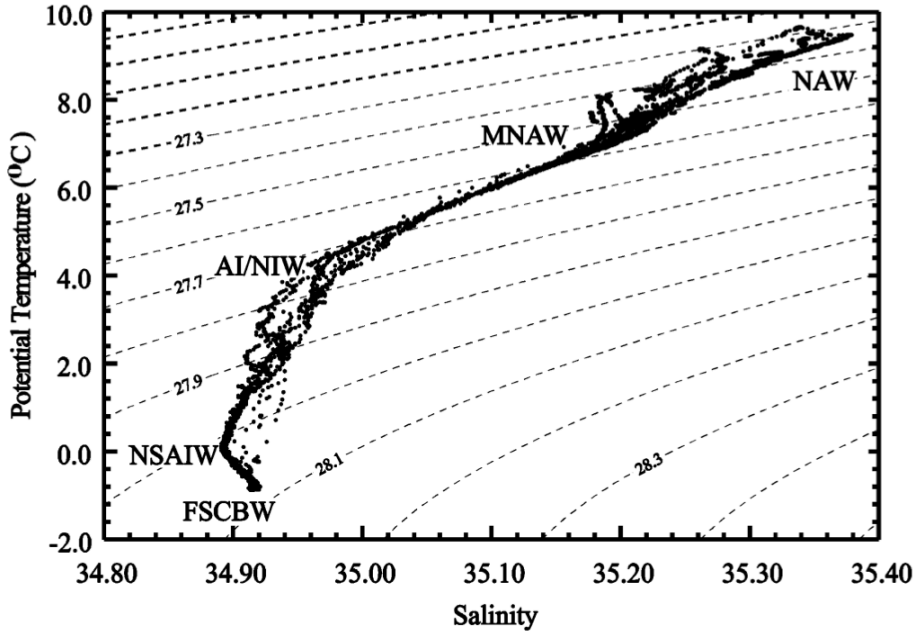

Figure 4 Typical temperature-salinity diagram from the Faeroe-Shetland Channel. The isopycnals show constant density (figure from Turrell et al., 1999).

Conductivity-temperature-depth data, or CTD-data, was collected near the core site of JM11-FI-15GC at the coordinates 62°45,79981N and 02°26,56193W. The data was collected on May the first 2011 and it spans 1129.7 meters. The data shows decrease in temperature and salinity with increased depth, but increase in density.

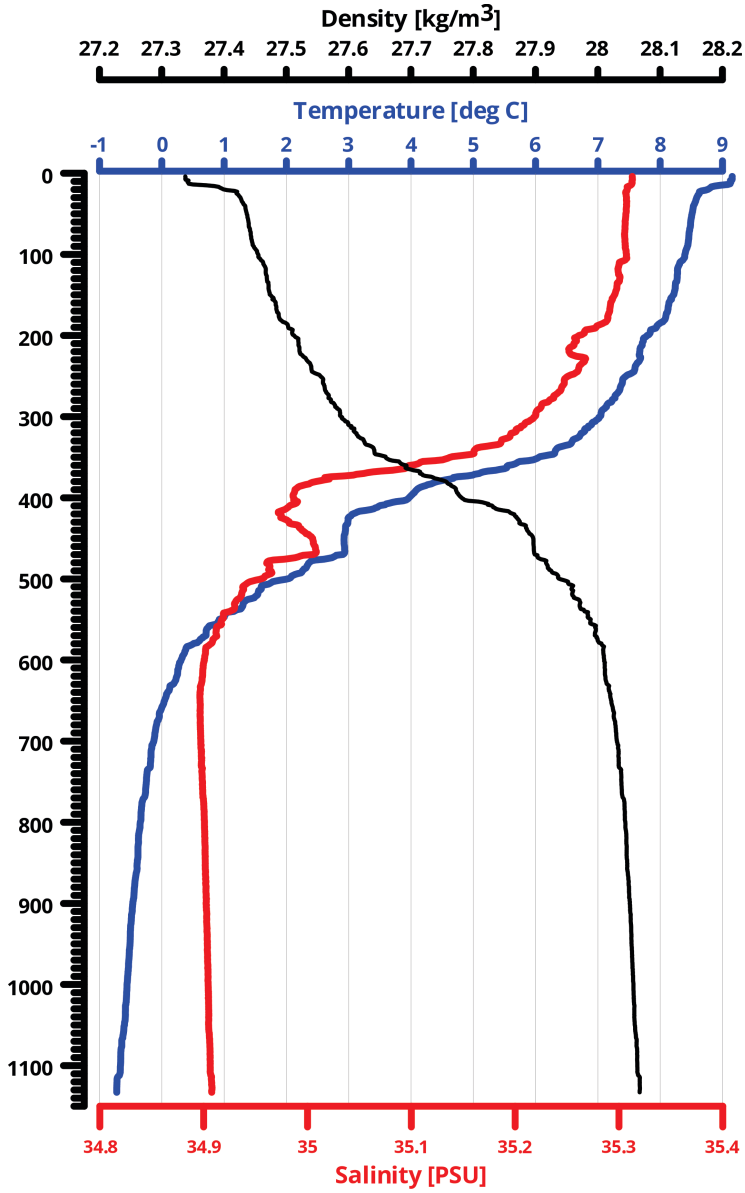

Figure 5 The CTD data from 1. May 2011

1.4 Dansgaard-Oeschger events

The Greenland Ice Core Project (GRIP) and the North Greenland Ice Core Project (NGRIP) have proven to be of great use in climate reconstruction. These ice cores contain detailed information of atmospheric conditions that spans the Holocene, the Weichselian glaciation and part of the last interglacial, the Eemian. The oxygen isotopes of these cores show twenty-four abrupt changes in temperature, termed Dansgaard-Oeschger events (D-O events) (Figure 6). These are interstadial, warm periods, followed by colder stadials (Andersen et al., 2004). They are very abrupt climate changes with abrupt warming that can occur within a few decades. This is very contrasting to the

Holocene, which seems to be quite stable in comparison (Dansgaard et al., 1993). Changes in ice volume are reflected in the marine $\delta^{18}O$ records (Hays et al., 1976). These rapid oscillations are found within the $\delta^{18}O$ records of the Greenland ice sheet, and are primarily caused by temperature during the ice formation (Dansgaard et al., 1993).

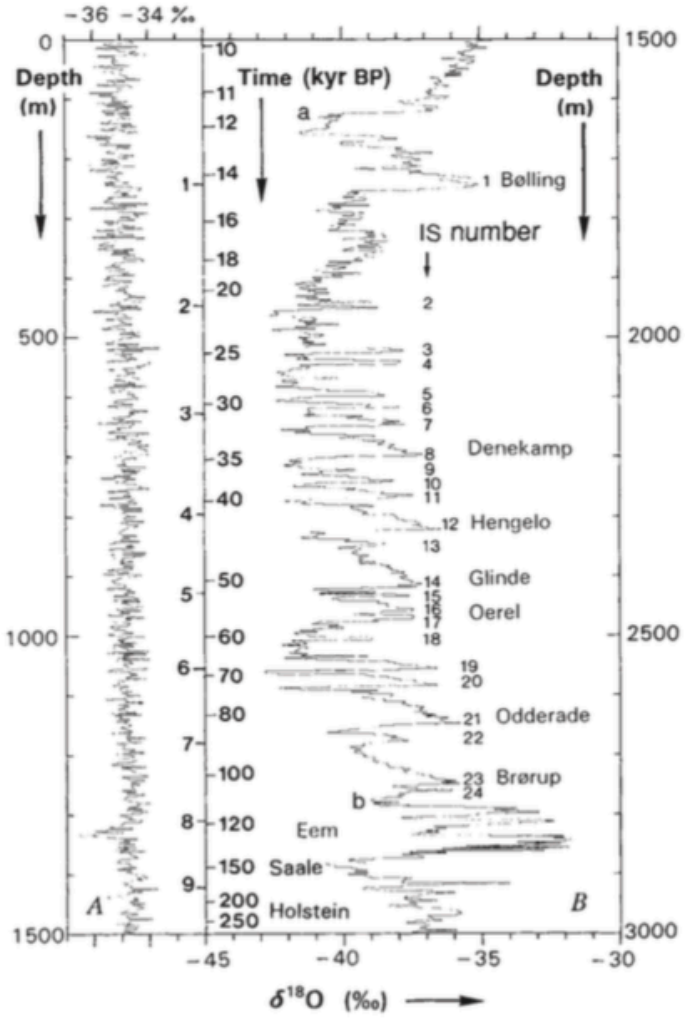

Figure 6 (A) First 1500 meters of $\delta^{18}O$ record from GRIP ice-core (B) Interstadials are marked on the figure by IS numbers and show abrupt change in $\delta^{18}O$ values (figure from Dansgaard et al., 1993)

Bond et al. (1993) noted that these D-O events found within the Greenland ice form a bundle, which last typically for 6000 - 10,000 years. These bundles, or Bond cycles, show a gentle cooling trend and they end abruptly with warmer temperature, for that reason they are referred to as asymmetrical saw tooth shapes by the authors. Each of these Bond cycles ends with a catastrophic release of icebergs into the North Atlantic, or so called Heinrich events. Heinrich events occur during times of extreme cooling. These D-O events are also found within the marine records (Bond et al., 1993).

1.5 Heinrich events

Heinrich (1988) originally described and identified six distinct layers that were characterized by large influx of ice rafted detritus (IRD). IRD is sediment that is displaced by ice. The sediment is carried within the ice, and as the ice melts the sediment is released. IRD can be carried a long way if the circumstances are favorable for ice transport (Hemming, 2004), but it is also a function of where the sediment is lodged within the ice (Andrews, 2000). Alley and MacAyeal (1994) approximated the mass of IRD of a typical Heinrich layer to be $1.0 \pm 0.3 \times 10^{15}$ kg.

Heinrich layers and smaller IRD layers were deposited between 14,000 and 70,000 years ago (Bond et al., 1992). During the last glaciation these layers were deposited approximately every 1000 - 2000 years (Bond and Lotti, 1995). These layers, including Heinrich layers, can be correlated to the stadials of the D-O events found within the Greenland ice cores, indicating that these events are connected (Bond and Lotti, 1995). Heinrich layers are spread across the whole North Atlantic region, with highest deposition between latitude 43°N and 53°N, and centered on the latitude 47°to 51°N (Ruddiman, 1997). Grousset et al. (1993) noted that icebergs during the Heinrich events melted along the southern margin of a large cyclonic gyre covering the northern Atlantic Ocean during the glacial period. Approximately 70 % of all the IRD deposited during the Quaternary is found in the subpolar North Atlantic south of Iceland (Ruddiman, 1977).

In IRD the sand-size fraction of the sediment is of focus, because the finer fractions can be transported by other means than ice rafting, either by sea ice or icebergs (Hemming, 2004). Within the layers there can be found high abundance of detrital carbonate, from limestone and dolomite. Geochemical analyses have shown that the most likely source for the detrital carbonate is bedrock in Hudson Bay and Hudson Strait (Bond et al., 1992). This indicates that these layers were formed from material brought in by massive discharges of icebergs from the Laurentide ice sheet (Hemming, 2004). This can been shown by that the detrital carbonate is thicker further west, closer to eastern Canada. This IRD carbonate can be found over more than 3000 km^2, which indicates very cold climate at that time allowing for further spreading of icebergs (Bond et al., 1992). The material in these events did not only originated from Canada, but there

is also material from Iceland and Greenland present (except in H3) (Grousset et al., 1993).

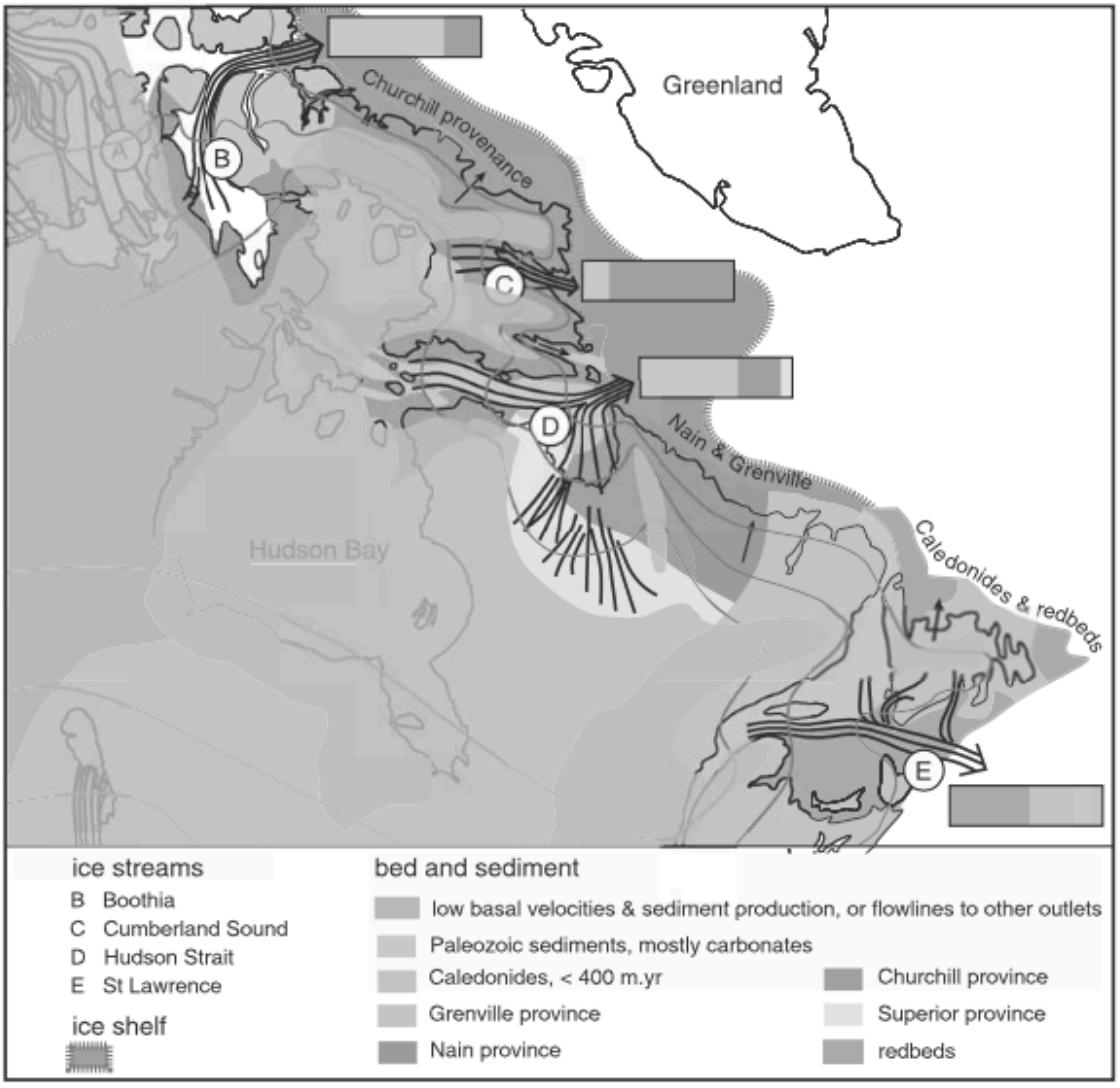

Figure 7 Part of the Laurentide ice-sheet, which covered large part of northern America during Pleistocene. Geochemical research has shown that high amount of IRD during Heinrich events came from Hudson Bay and Hudson Strait (figure from Hulbe et al., 2004).

The magnetic susceptibly signal is stronger for ice rafted detritus than biogenic carbonate, and for that reason it can be helpful for investigation of ice-rafting events of the Pleistocene glaciations. The ice rafted detritus is of terrigenous origin and is often rich in magnetic minerals, giving high magnetic susceptibility values. Heinrich events are catastrophic IRD events that have extremely strong magnetic susceptibility signal, and can therefore be used for correlation purposes (Robinson et al., 1995). However, in vicinity of the Faeroe Islands the magnetic susceptibility is low during the stadials, but

high in interstadials, due to differences in origin of the material (e.g. Rasmussen et al., 1996b).

These events are also distinguished by higher abundance of the cold surface water foraminiferal species *N. pachyderma* (s) (Heinrich, 1988). The tests of the foraminifera in these layers are usually well preserved (Broecker et al., 1992). These foraminifera indicate colder surface waters; also within their test the $\delta^{18}O$ measurements indicate lower salinities of the surface (Bond et al., 1992).

1.5.1 Theories behind the cause of Heinrich events

The driving force behind the Heinrich events is not fully understood to this day. There are both internal theories (MacAyeal, 1993; Alley and MacAyeal, 1994), and external theories (Johnson and Lauritzen, 1995; Hulbe, 1997; Hulbe et al., 2004).

Binge purge model

This binge/purge model is one of the models trying to understand the force behind this large release of icebergs from the Laurentide ice sheet. The binge/purge oscillation could have been the reason for the 6000 - 10,000 year intervals (Alley and MacAyeal, 1994). The idea behind the Binge/purge model, as proposed by MacAyeal (1993), is that is not externally forced, rather it has to do with internal forcing of the Laurentide ice sheet. The binging phase correlates to growing of the ice sheet to a large size. The purging phase is when the ice sheet starts to move on the lubricated substrate, ending with the release of huge amount of icebergs (MacAyeal, 1993).

The rate of snow accumulation on the ice sheet controls the pace of the episodic behavior. In the growing/binging phase the substrate is thought to have been frozen, thus allowing the ice sheet to grow. Eventually this phase reaches its threshold, it is when the ice sheet becomes warm-based, and this phase is the purging phase, when the ice sheet starts to move. This thawing could be a result of advection of heat, geothermal heat or friction. The thawing substrate can be easily eroded into a slippery lubricant, as it is made from soft Paleozoic carbonates and Cretaceous mudstone (MacAyeal, 1993). The purging phase can last up to 750 years. When the ice sheet has become quite thin, the substrate freezes again, thus the binging phase can start again (Figure 8) (Alley and MacAyeal, 1994).

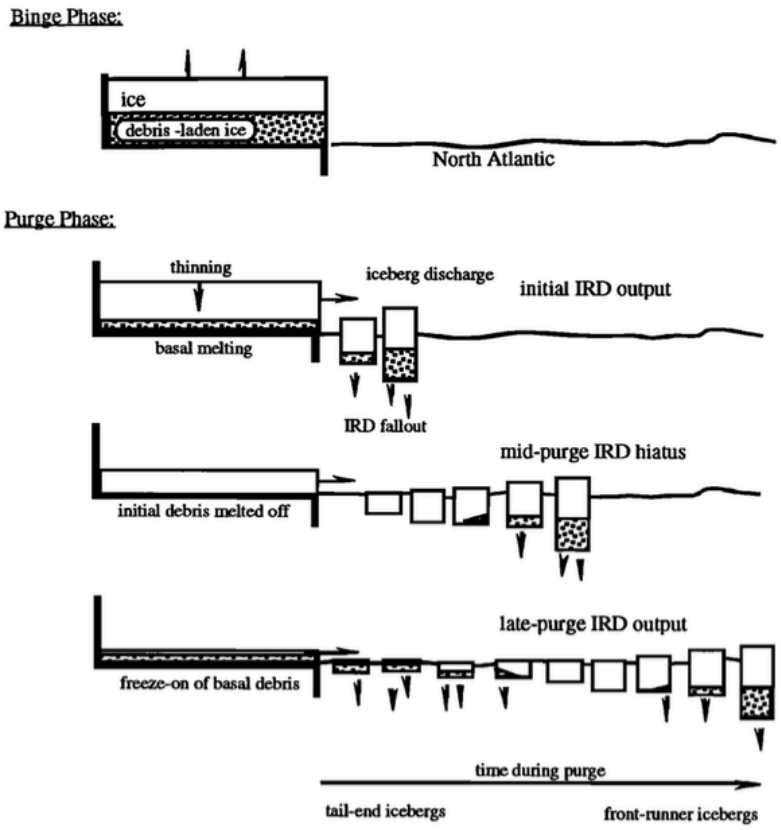

Figure 8 shows simplified diagrams of the processes that might have triggered the Heinrich events. Binge phase represent the growing state of the Laurentide ice-sheet until it reaches the threshold and starts purging (figure from Alley and MacAyeal, 1994).

Hulbe (1997) states that this theory provides explanation for the increase of carbonate IRD, but it is not good enough to explanation the co-occurrence for the Heinrich events and the smaller cold (high points) events of D-O cycles (Hulbe, 1997). Also in Hulbe et al. (2004) they say that this theory would not explain why sediments from other places, such as Iceland and Europe (glacial regime), would also be present in the same IRD layers as from Canada. It is therefore more likely that the Heinrich events are connected to external, not internal forces (Hulbe et al., 2004). Snoeckx et al. (1999) also indicates that the European ice sheets could have surged before the North American ice sheet did.

Hudson Bay- Hudson Strait jökulhlaups

A different hypothesis about the formation of the Heinrich events comes from Johnson and Lauritzen (1995). This hypothesis is based on repeated jökulhlaups from a large lake, Zissaga, barricaded with ice. This large lake was formed in the Hudson Bay, and it was barricaded by ice from the mouth of the Hudson Strait. A large jökulhlaup could

have large effect on cooling of the climate from massive surges. The melt water from icebergs would lower the salinity of the ocean and it would have large effect on the deep water formation. They argue that smaller jökulhlaups, than the ones that could have caused the Heinrich events, could be the reason for the D-O cooling cycles (Johnson and Lauritzen, 1995). But Hemming (2004) indicates that it is doubtful that a large lake would be present in Hudson Bay at the Last Glacial Maximum, but perhaps during earlier phases of ice sheet buildup.

Catastrophic ice shelf breakup

This theory argues that the formation of Heinrich layers is instead connected to ice shelf build up and break down (Hulbe, 1997). This theory is solely based on external climate forcing. Even though there is not a Heinrich event for every cold D-O event, they are thought to be connected to longer-lasting cold intervals (Hulbe, 1997).

This theory was improved by Hulbe et al. (2004), by using data from the break-up of the Larsen A and B ice shelves from Antarctica. The idea behind the break-up is that long period of gradual warming can cause a catastrophic event. There were crevasses on the ice shelves, which filled with water during the summer melt periods. Since water is denser than the ambient ice, the water can act as wedge causing strain on the ice. Eventually the shelves reach their threshold and can suddenly release large amounts of icebergs into the ocean (Hulbe et al., 2004).

Hulbe (1997) suggest four stages how this process could form the Heinrich events. The first stage would be a period of cooling, which causes the growth of the Laurentide ice sheet. The second and third stage has to do with freeze on, which occurs when the cooled melt water from underneath the ice sheet rises up because of buoyancy, and freezes again on the ice shelf. This process can protect the basal sediment, which can otherwise be prone to melting out (Hulbe et al., 2004). The basal ice is enriched with carbonate sediments. The final stage is when the temperature gets warmer in the end of the D-O events, which causes the ice sheet to retreat and the formation of icebergs ends (Hulbe, 1997). This course of events is illustrated in Figure 9.

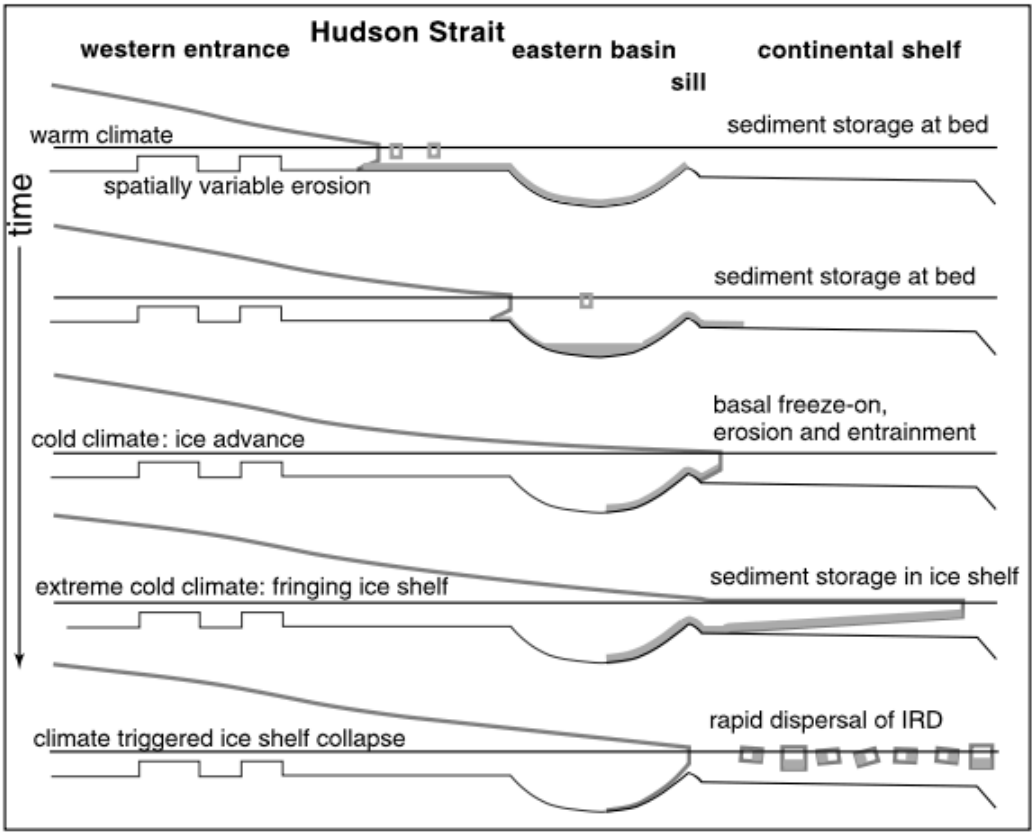

Figure 9 Conceptual model of Hulbe (1997) and Hulbe et al. (2004) for the cause of Heinrich events. The ice sheet grows in increasing cold climate and the basal ice stores large amounts of IRD within. Eventually the ice-sheets breaks up, dispersing large amounts of icebergs. Many of the fragments of the ice-sheet will capsize, helping it even further to spread over larger area (figure from Hulbe et al., 2004)

2 Materials and methods

The core JM11-FI-15GC was taken among 10 other gravity cores during a scientific cruise that took place between 26th of April to 11th of May 2011. The ship that was used in this expedition was the university's ship then named R/V Jan Mayen, later R/V Helmer Hansen. Core JM11-FI-15GC was cored the 1st of May 2011 at Fugløy Ridge at the coordinates 62°45,68488N and 02°27,78388W. The core was 583.5 cm long and from a water depth of 1119.8 m (Rasmussen and Nielsen, 2011).

2.1 Sediment coring

R/V Jan Mayen is fully equipped to take gravity cores as well as other types of cores. The gravity corer on board has a 6 m long steel barrel with inner diameter of 11 cm. It weighs in total 1900 kg (Rasmussen and Nielsen, 2011). The instrument is lowered through an opening in the ship's hull, using winches. The gravity corer is ideal for sub-seafloor sampling, and as the name suggest, the gravity helps the gravity corer to penetrate the sediment. The 6 m long barrel has a plastic liner inside for sediment sampling and a core cutter at the end, allowing it penetrate the seafloor. A core catcher is placed inside the plastic liner. The catcher allows the sediment to come into the plastic liner, and prevent that it falls out when the gravity corer is raised up from the sea floor. After the gravity corer has been winched back from the ocean, it is placed horizontally so the liner can be pulled out. The plastic liner is then pulled out, marked and sawed into 1 m sections and stored at 4°C.

2.2 Multi-Sensor Core Logger

The core was logged by a Multi-Sensor Core Logger (MSCL) 10th of June 2011. The MSCL measured gamma density, P-wave velocity, magnetic susceptibility, resistivity, X-ray fluorescence and natural gamma measurements (Geotek, 2014).

Magnetic susceptibility

Magnetic susceptibility (MS) is the measurement of magnetization of the sediments. The MS is sensitive to temperature so the core is usually taken to the laboratory the day

before to get to room temperature. The core JM11-FI-15GC was measured using a Bartington MS2-loop sensor every 1 cm for 10 seconds.

2.3 Opening of the core

Based on the MS record, the core intervals containing sediments correlating with Heinrich event H4 and Greenland interstadial 8 were selected. Core sections 3 and 4, (200 - 400 cm below the sediment surface) were opened 30th January 2014. A circular saw was used to cut the plastic liner. A wire string was pulled through the core sections to split the two halves from each other. One of the halves was marked as 'Archive', wrapped in plastic and put in storage at 4 °C, while the other half was marked as 'Work'. The surface of the working half was cleaned and visually described. Color was described based on the Munsell Soil Color Chart.

2.3.1 Sample preparation

After the core sections had been descripted, the parts of the core sections that were to be included in this study were cut into 1 cm thick slices (200 - 309 cm). To make the cutting easier an Osmotic knife was used. Material closest to the core liner can be disturbed in the process of drilling; therefore the outermost sediment of each slice was discarded. A total of 109 samples were collected, and in each samples foraminifera, IRD, tephra and foraminiferal test fragmentation were counted.

The samples were then placed in pre-weighed plastic-bags, weighed and stored in a freezer until they could be placed in the freeze-dryer, Christ Alpha 1-4. The freeze-dryer vaporizes the water from the samples from ice to vapor, without melting first. This process is less destructive for the foraminifera than drying in an oven. After the samples had been dried, they were weighed again. By knowing the wet and dry weight it is possible to calculate the water content.

2.4 Sieving

The samples were wet sieved over four sieves with mesh sizes 1 mm, 250 μm, 100 μm and 63 μm. The residues were extracted from the sieves into filter paper, using distilled water from a bottle. The residues in the filters were placed in an oven at 40 °C until they

were completely dried. Between each sieving the sieves were first cleaned with running water and then put in a sonic batch for a few minutes. The sieves were then removed from the sonic bath; cleaned again with running water and finally compressed air was used to blow out any remaining sediment. The dry residues were weighed and put in small glass containers marked with core name, depth, and mesh size used.

2.5 Ice rafted detritus

IRD was counted in the size fractions >1 mm and 250 μm – 1 mm in 109 samples at the interval 200 - 309 cm. In the size fraction >1 mm everything was counted. In the size fraction 250 μm – 1 mm everything was counted, when there were few IRD grains to be found. Some samples had quite a large number of IRD grains and therefore 200 – 300 grains of IRD was picked. The concentrations of IRD in the two size fractions were calculated as number of grains per gram dry weight sediment. After the IRD had been counted, the residues in the size fraction 250 μm – 1 mm was put back into the glass container with the 100 μm size fraction for the counts of foraminifera (see below).

2.6 Tephra

The tephra particles found within the sample residues were divided into two groups; the first being light porous particles that could have been carried by the wind, the second being the heavier, solid particles that would be more likely to have been carried by oceanic currents or ice rafted (blocky particles). The tephra grains were counted semi-quantitatively in the size fractions >1 mm, 250 μm – 1mm and 100 – 250 μm. In the >1 mm size fraction all tephra particles were counted, in the 250 μm – 1 mm tephra found within the squares counted for IRD were counted. In the 100 – 250 μm size fraction the tephra found within the squares of counted foraminifera were counted.

2.7 Foraminifera

Foraminifera were identified in the size fraction >100 μm (see above). There was no foraminifera found in the >1 mm size fraction. A splitter was used to divide the residues into two halves. Some samples needed to be split more than once due to their size. The splitter was always cleaned thoroughly with compressed air before and after use.

Each sample was spread evenly over a metal tray. The tray consists of 45 identical sized squares. Squares were picked at random until at least 300 of both benthic and planktonic foraminifera were counted. The foraminifera were identified to species level and percentages calculated. A total of 109 samples at 200 - 309 cm were used for foraminifera identification.

2.8 Foraminiferal test fragmentation

Fragments of planktonic foraminiferal tests were counted semi-quantitatively in the same random squares as the foraminifera were counted and identified. These fragments mostly came from *Neogloboquadrina pachyderma* sinistral (s) as might have been expected, since it is the most common foraminifera found in this core (see below). A simple equation of fragmentation was used:

$$\frac{no.fragments}{no.fragments + no.whole\_forams} \cdot 100 = fragments\%$$

2.9 Stable Isotopes $^{18}O/^{16}O$ and $^{13}C/^{12}C$

N. pachyderma (s) was used for analyses of the oxygen and carbon isotope in their shells. Every other centimeter was picked from the cores from 200 to 309 cm. A total of 20 - 30 specimens of *N. pachyderma* (s) were picked. The foraminifera were undamaged and contained no visible contamination. They were all similar in size and close to the ideal square-shape with four chambers in the last coil. The samples were analyzed at the Geological Mass Spectrometer Laboratory at the University of Bergen using a Finnigan MAT 253 mass spectrometer with a Kiel IV device at with a precision ± 0.06 ‰ for $\delta^{18}O$ and ± 0.03 ‰ for $\delta^{13}C$.

2.10 Radiocarbon dating

Five samples were sent to the ^{14}Chrone Centre, Queen's University, Belfast, United Kingdom. All of the samples were exclusively the planktonic species *N. pachyderma* (s). An accelerator mass spectrometer (AMS) is used in the laboratory. It measures the number of ^{14}C relative to ^{12}C and ^{13}C. Due to reservoir effect all of the samples were calibrated to calendar years BP using Fairbanks Calibration curve.

Reservoir effect

The Fairbanks calibration program was used to calibrate for the reservoir effect. The calibration is done because the ^{14}C age is not the same as calendar age, for various reasons. Due to unknown reservoir age during the time interval, 400 years in reservoir age was subtracted.

3 Foraminifera

Foraminifera are very useful in paleoceanography and paleoclimatology research due to their small size and abundance. They are found in a wide range of marine environments, where their test can make up large amounts of the sediments. The change in fauna assemblages can be very beneficial for environmental studies as many species have very strong environmental preference, such as very low tolerance to change in salinity, temperature, depth, nutrients or turbulence (Armstrong and Braiser, 2009). Ecological preferences of living modern foraminifera are used to interpret the fossil record of foraminifera.

3.1 Planktonic foraminifera

Planktonic foraminifera live in the surface layers of the ocean where most of them reproduce. The major factors controlling their species abundance are temperature and salinity. The foraminifera are therefore great for elucidating variations in past oceanic temperature (Armstrong and Braiser, 2009).

Neogloboquadrina pachyderma (Ehrenberg, 1861)

There are two forms of *N. pachyderma* found in core JM11-FI-15GC, dextral (right coiled) and sinistral (left coiled). This is not just a morphological difference between the forms, but there is a large genetic difference between them, enough that they should be considered to be two different species. However, there is around 1 - 3 % aberrant coiling found in both species (Darling et al., 2006). *N. pachyderma* (s) has an optimal sea temperature around 0 °C and is considered to be a polar species. The *N. pachyderma* (d) (now named *N. incompta* (Darling et al., 2006)) is considered to be subpolar with optimal sea surface temperature around 12 °C (Schmidt et al., 2004). Each species has therefore a strong correlation with surface water temperature.

Other planktonic foraminifera

Globigerina bulloides (d'Orbigny, 1826), *Globigerina glutinata* (Egger, 1895), *Globigerinita uvula* (Ehrenberg, 1861) and *Turborotalita quinqueloba* (Natland, 1938) are associated with warm and saline Atlantic Water (Jenning et al., 2004).

3.2 Benthic foraminifera

Benthic foraminifera are found in practically all-marine environments (Linke and Lutze, 1993). They are bottom-dwellers, that can live as epifaunal or infaunal (shallow, middle or deep). The dominant factors controlling their abundance are temperature, salinity, organic matter, light and substrate (Armstrong and Braiser, 2009).

Astrononion gallowayi (Loeblich & Tappan, 1953)

A. gallowayi is an epifaunal species that prefers environments with low temperatures (<1 °C) and high salinities (>30 ‰). It prefers substrates with coarse sediments (Steinsund et al., 1994; Polyak et al., 2002), and is prone to inhabit shallow areas (Steinsund et al., 1994; Jennings et al., 2004). The species often occurs together with *C. lobatulus*, showing a preference for strong bottom currents (Polyak et al., 2002).

Cassidulina reniforme (Nørvang, 1945)

C. reniforme is an arctic species (Mudie et al., 1984), associated with near glacial environments, sediment loaded waters and high turbidity (Hansen and Knudsen, 1995), but does not tolerate as high a turbidity as *E. excavatum* f. *clavatum* (Steinsund et al., 1994). It is infaunal and lives in the uppermost centimeters (Hunt et al., 1993), in silty muds and usually shallower than 100 m water depth in the Arctic region (Mudie et al., 1984). *C. reniforme* indicates environments that are characterized by glacial-marine sediments (Scott et al., 1984). It prefers low temperatures (Hald and Korsun, 1997) and environments with salinity ≥30 ‰ (Polyak et al., 2002). Furthermore, *C. reniforme* is believed to be an indicator of 'warm' glacial margins, where the sea temperature is relatively high (Scott et al., 1984). Jennings and Helgadóttir (1994) note that this species is likely an indicator of Atlantic Intermediate Water in the Nordic Seas.

Cassidulina neoteretis (Seidenkrantz, 1995)

C. neoteretis thrives in cold bottom waters (-1 °C) with optimal salinity between 34.91 – 34.92 ‰. It is found in various glacio-marine environments – an always cold environment. *C. neoteretis* is a deep-water shallow-infaunal species, often found in environments with a fine-grained organic rich mud (Mackensen and Hald, 1988; Steinsund et al., 1994). It is considered an indicator of Atlantic Intermediate Water in

the Nordic Seas (Jennings and Helgadóttir, 1994). It dominates during stadials intervals at the Faeroe Margin (Rasmussen et al., 1996).

Cibicides lobatulus (Walker & Jacob, 1798)

C. lobatulus is epifaunal species that clings to exposed surfaces such as rocks or algae (Steinsund et al., 1994). It thrives in coarse substrates with strong bottom currents (Hald and Steinsund, 1996; Steinsund et al., 1994). It tolerates a wide range of temperatures with a normal salinity. It is found in high numbers in coastal areas and in banks where the salinity is ≥32 ‰ (Steinsund et al., 1994)

Elphidium excavatum (Terquem, 1875)

More than one subspecies of *E. excavatum* are known (Feyling-Hanssen, 1972), but these were not distinguished into subspecies in this thesis. *E. excavatum* is a post glacial species, i.e. most common in late glacial or post glacial periods. It can live in wide range of temperature and salinity (Vilks, 1981), but prefers arctic conditions (<1°C) with a reduced bottom water salinity (30 - 34 ‰) (Steinsund et al., 1994). Alve and Murray (1999) noted that it tolerates a number of substrates, from coarse silt to very coarse sand. It also can live in a wide range of depths (Scott et al., 1984). It is an opportunistic species, i.e. extremely adaptable with changes in environmental conditions (Linke and Lutze, 1993). It is often found in intervals where there is a low concentration of foraminifera (Steinsund et al., 1994). This species is often found in the narrow interval between the stadials and the interstadials, and in cooling intervals (Rasmussen et al., 1996b). This species seems to dominate in environments with low temperatures, salinities and in the presence of sea ice (Steinsund et al., 1994).

Epistominella vitrea (Parker, 1953)

E. vitrea is an opportunistic species known to tolerate low oxygen levels (Gustafson and Nordberg, 2001). The abundance of organic matter is a very important factor for its prevalence. It is a deep infaunal species that can migrate upwards, when conditions are favorable (Ernst et al., 2005). It is found on the lower-slope and upper-rise in the Labrador Sea, where it is influenced by the Norwegian Sea Overflow water mass (Schafer and Cole, 1982). Rasmussen et al. (1996b) suggest *E. vitrea*'s occurrence near the Faeroe-Shetland Channel might be connected with an unstable food supply.

Melonis barleeanus (Williamson, 1858)

M. barleeanus is a deep-water (Caralp, 1989) intermediate infaunal species that lives in a muddy substrate, where it depends on a relatively steady supply of partly degraded organic matter for nourishment (Caralp, 1989; Jennings et al., 2004). It is highly adaptable to environmental changes, and if needed, can change from infaunal to epifaunal (Linke and Lutze, 1993). It prefers salinities of more than 32 ‰ (Steinsund et al., 1994). This species is abundant during interstadials intervals in the Faeroe Margin (Rasmussen et al., 1996b).

4 Results

The most important results from core JM11-FI-15GC will be presented in this chapter. The data will be divided into three intervals; interstadials, transitional cooling intervals and stadials as seen in Rasmussen et al. (1996b) and Fronval et al. (1995). This pattern is very clear in the data of core JM11-FI-15GC and therefore the record will be presented, interpreted and discussed based on these intervals (Figure 10), except for the tephra record.

Stadials are characterized by large decrease in $\delta^{18}O$, high concentration of IRD, and the planktonic foraminifera *N. pachyderma* (s) dominates the foraminifera population (Bond et al., 1992; 1993). The magnetic susceptibility is also low during stadials (Rasmussen et al., 1996b). Interstadials have higher values of $\delta^{18}O$ and relatively low concentration of IRD. Interstadials have higher magnetic susceptibility than stadials (Rasmussen et al., 1996b) (Figure 10).

Changes in $\delta^{18}O$ values are used to correlate marine sediments to Greenland interstadials found in ice-cores (Bond et al., 1993). As there were not $\delta^{18}O$ values for the whole core, just a small interval (200 - 309 cm), magnetic susceptibility was used for correlation purposes instead (Figure 18). The magnetic susceptibility shows a clear asymmetrical saw tooth pattern (Figure 10). The pattern corresponds to D-O events, which show higher values at interstadials (Rasmussen et al., 1996b). To identify the D-O events by number, the magnetic susceptibility of the core was compared to values from the high-resolution piston core ENAM93-21 from Rasmussen et al. (1996b). In the interval of interest, four D-O climatic events were identified. The largest and most conspicuous event of high magnetic susceptibility values corresponds to the Greenland interstadial 8 (GI8). The stadial before GI8, corresponds to Heinrich event 4, as seen by Figure 20.

The GI8 was divided into two parts, the lower corresponds to the peak interstadial interval and the upper with decreasing magnetic susceptibility values to the transitional cooling interval. The lower part (274 – 254 cm) has high values of magnetic susceptibility, high $\delta^{18}O$ and a low concentration of IRD. The upper part (253 – 230 cm) was termed 'transitional cooling period' (Johnsen et al., 1992; Rasmussen et al., 1996), and was identified by decreasing magnetic susceptibility and increasing IRD

concentration (Figure 10). The three largest events will be used as a template for the smaller D-O events and will be described in the results. These three events are very well defined and the smaller events clearly follow their trend in the data (Figure 10).

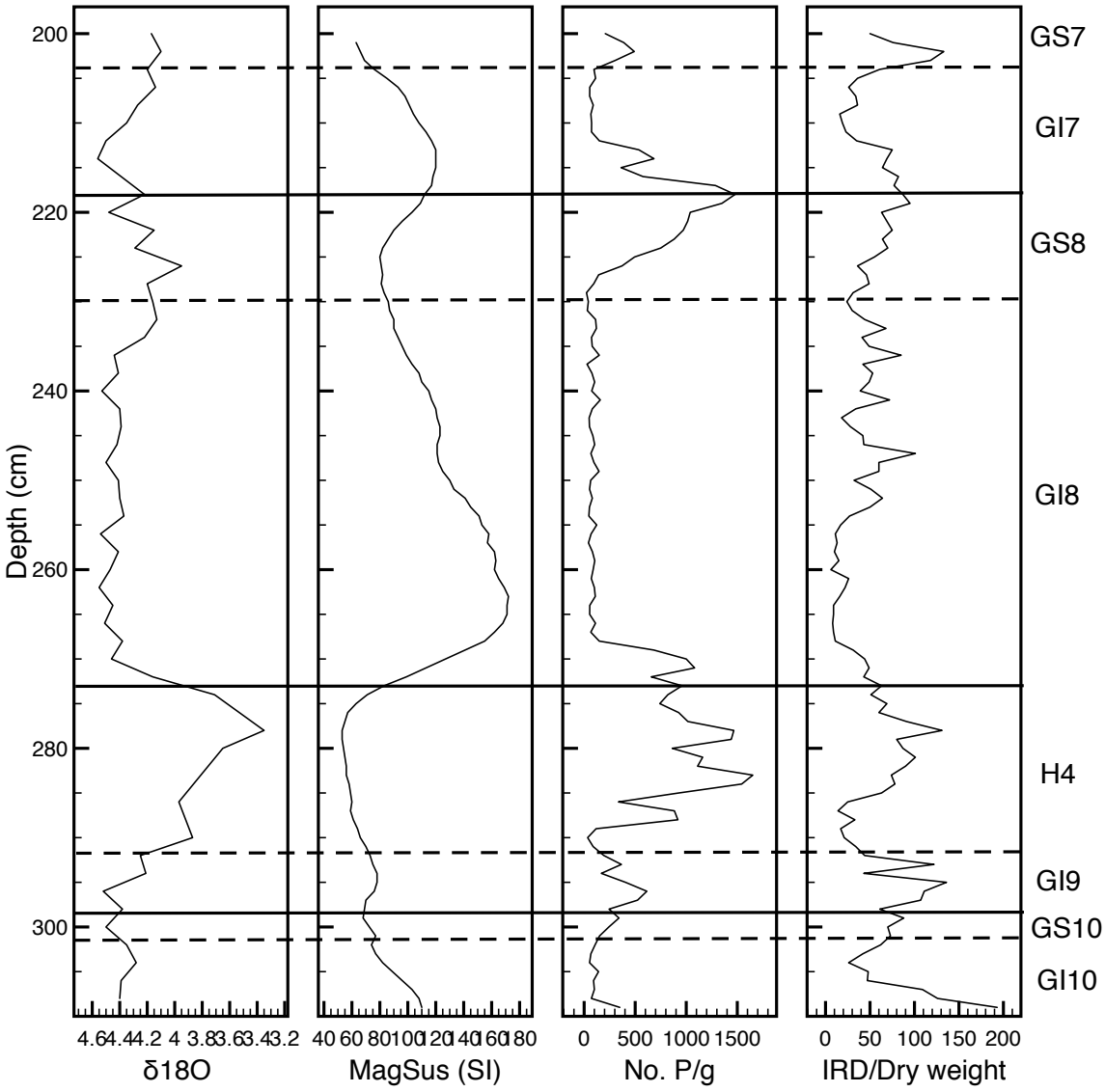

Figure 10 Comparison of $\delta^{18}O$, magnetic susceptibility, concentration of planktonic foraminifera and ice rafted detritus per gram dry weight. The data was used to determine the division into stadial/interstadial intervals. The dashed lines mark the starting points of the stadial intervals/Heinrich event and solid line mark the start of interstadials. Transitional cooling intervals are part of the interstadial intervals in this figure.

In total 67 species of were foraminifera identified. When agglutinated species were found, they could not be separated into species due to the bad preservation. Few foraminifera were classified as "other", either due to bad preservation or because of

difficulties in identifying to a species level. The most important and/or most common species will be presented here.

Only six species of planktonic foraminifera were identified in the core: *N. pachyderma* (s), *N. pachyderma* (d), *Globigernia bulloides, Globigerinita glutinata, G. uvula and Turborotalita quinqueloba.* Only the first two are of interest due to scarcity of the other three and bad preservation (Figure 25 in Appendix). The *N. pachyderma* (s) and *N. pachyderma* (d) show fluctuations through the whole section, but *N. pachyderma* (s) is always dominant among the planktonic foraminifera. *N. pachyderma* (s) values fluctuate between 91.21 – 100 % of the total planktonic foraminifera.

4.1 Interstadial interval ~ 274 – 254 cm

Description

The interval appeared to be fine grained with no visually noticeable change in grain size. The color was grayish brown (3/2) according to Munsell Soil Color Chart.

Grain size distribution

The percentage of 63 - 100 μm increases through the interval and averages at 55.22 %. The next size fraction 100 - 250 μm has 37.93 %, 250 μm – 1 mm makes up 5.32 % and >1 mm makes up only 1.52 %. As seen in Figure 11 the water content is relatively higher during interstadial intervals with 42.32 %. The IRD concentration decrease in the interval but averages 23.90 IRD/g.

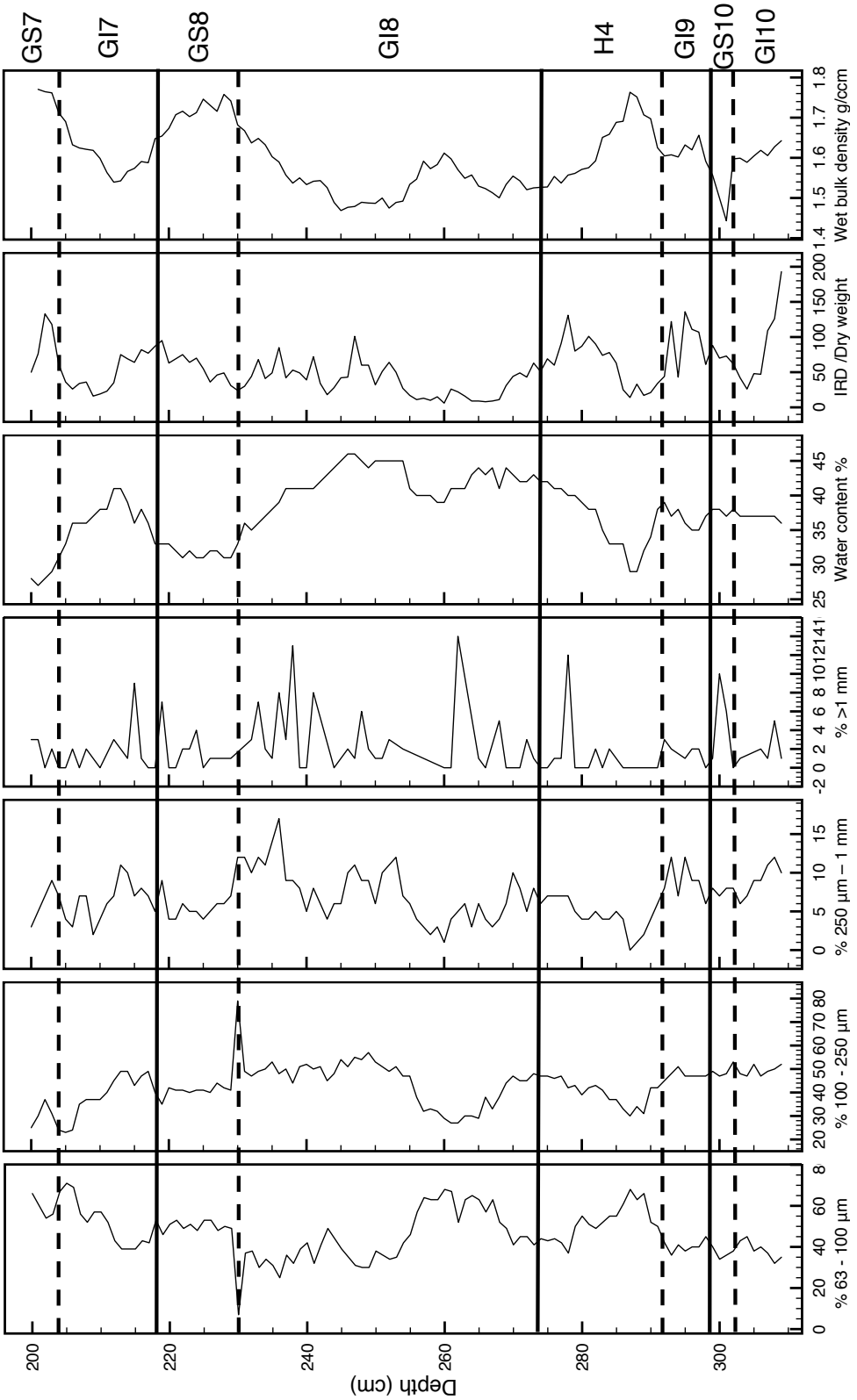

Figure 11 Sediment characteristics of core JM11-FI-15GC.

Multi-Sensor Core Logger data

The start of the interstadial GI8 is marked by abrupt increase in the MS values (Figure 10). The GI8 is a large event and reaches a maximum at 263 cm with 172.51 SI. However, the wet bulk density value is not clear, but it seems to be low (1.55 gm/cc) during the interval.

Planktic $\delta^{18}O$ and $\delta^{13}C$ values

The interstadial starts with an abrupt increase in the planktic $\delta^{18}O$ and $\delta^{13}C$ values measured in *N. pachyderma* (s). From 274 – 254 cm the value changes from 3.71 ‰ to 4.37 ‰. Looking at the same interval for $\delta^{13}C$ the value change from 0.12 ‰ to 0.33 ‰.

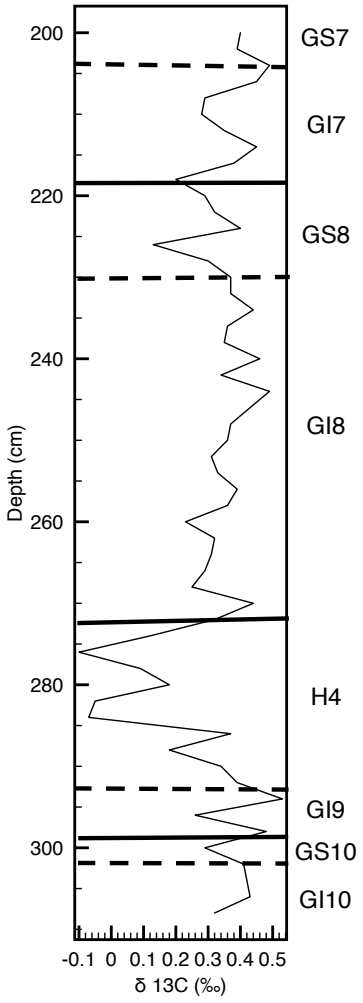

Figure 12 Changes in $\delta^{13}C$ values from 200 – 309 cm. The start of the stadials is marked by dotted line, the interstadials by solid black line

Foraminiferal test fragmentation

Figure 19 shows the fragmentation percentage from the 100 μm – 1 mm size fraction. These fragments are mostly from the planktonic species *N. pachyderma* (s), as that species is the most abundant in the record. Nearly all of the fragments appear to be of planktonic origin. During the interstadial interval there is an abrupt increase in the percentage of fragmentation with values over 70 %. The percentage of fragmentation averages at 65.61 %.

Foraminifera

There is a decrease in the concentration of foraminifera (440.10 Foraminifera/g) compared to stadials. This value is much lower than observed in the previous stadial interval. More planktonic (397.78 No. P/g) foraminifera are found than benthic (132.32 No. B/g). *C. neoteretis* (34.27 %) is the most common benthic foraminifera in the interval, however, its value has decreased from the previous stadial. There are very distinct peaks seen for *M. barleeanus* (24.75 %) and *C. lobatulus/A. gallowayi* (11.84 %). When their value starts to decrease there is an increase in *E. excavatum* (6.82 %). *C. reniforme* (3.92 %) does not show any large oscillation through this interval. In this interval *E. vitrea* (7.87 %) shows a very abrupt peak just before *M. barleeanus* peaks.

4.2 Transitional cooling interval ~ 253 – 230 cm

Description

The color was grayish brown (3/2) according to Munsell Soil Color Chart. No visual change was seen.

Grain size distribution

The transitional cooling interval has a lower percentage of 63 - 100 μm (34.87 %) relative to the other intervals. 100 - 250 μm (52.25 %) size fraction is the most common within this interval, with stable values. However, there is a very abrupt peak at 230 cm with values up to 79.42 %, this occurs at the boundary with a stadial. 250 μm – 1 mm makes up only 10.05 % however, the >1 mm size fraction has quite high percentages relative to interstadials with 2.82 %. The water content average is 41.78 %. The IRD concentration (49. 57 IRD/g) is quite unstable, and has a few abrupt peaks.

Multi-Sensor Core Logger data

During transitional cooling interval there are gradually decreasing values of MS. The wet bulk density is rising during this interval.

Planktic $\delta^{18}O$ and $\delta^{13}C$ values

There are some oscillation in the values of $\delta^{18}O$ and $\delta^{13}C$, but the values are relatively stable.

Foraminiferal test fragmentation

Foraminiferal test fragmentation is not much lower than during the interstadials, with values at 55.90 %.

Foraminifera

The concentration of foraminifera was lowest in the transitional cooling intervals (148.21 Foraminifera/g). There is also a decrease in the P:B ratio, which is 1.48 for the transitional cooling interval but 2.07 for the interstadial interval. *E. excavatum* (41.44 %) is the most common benthic foraminifera, and has high values throughout this interval. *C. neoteretis* has stable values and an average of 28.78 %. Other foraminifera have low values in this interval, i.e. *C. reniforme* (3.43 %), *M. barleeanus* (4.33 %), *C. lobatulus/A. gallowayi* (3.45 %) and *E. vitrea* has a very low value of 1.12 %.

4.3 Stadial intervals ~ 291 - 275 cm (Heinrich event 4)

Description

The main color of the core was relatively homogenous until the interval 299 – 273 cm, which corresponds with the H4. The color of this interval was gray (5/1) according to Munsell Soil Color Chart. This sudden color change was not noticed at other stadials.

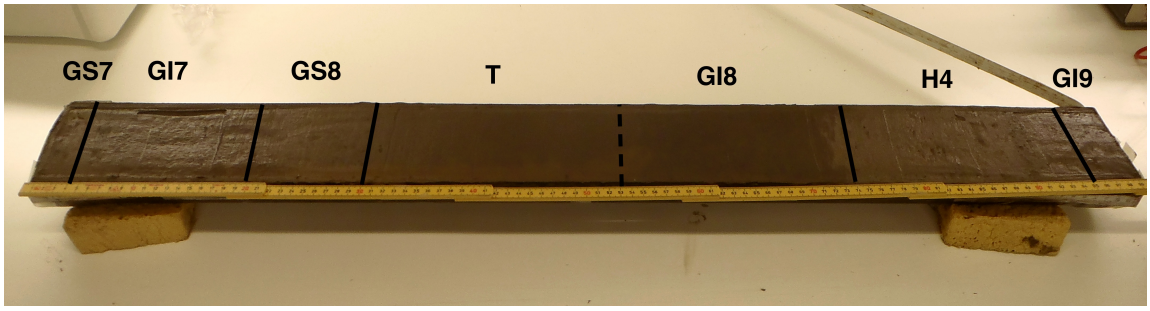

Figure 13 This is section 3, which is shows the largest events. H4 is marked by a sudden color change and stands out clearly. The marking "T" stands for transitional cooling interval and is part of the GI8, and therefore disguised from it by a dotted line.

Grain size distribution

The most common grain size in this interval is 63 - 100 μm (53.21 %), and the second most common is 100 - 250 μm (40.14 %). 250 μm – 1 mm is higher in stadials then the other intervals with 4.91 %. >1 mm has an average value of 1.73 %. The concentration of IRD increases in the beginning of the stadial, and averages at 63.39 IRD/g. Water content decreases in the stadial with values of 36.69 %, when the percentage of 63 - 100 μm increases.

Multi-Sensor Core Logger data

MS value slowly declines until bottom value is reached in the stadials. The lowest value is found in H4, only 53.94 SI. The density is not that clear, but there is an indication of higher values during the stadials. The wet bulk density averages 1.63 gm/cc.

Planktic $\delta^{18}O$ and $\delta^{13}C$ values

Stadials are characterized by low values of $\delta^{18}O$ and with very low values during H4. The stable oxygen isotope graph (Figure 10) shows that there is a slow increase of the lighter ^{16}O isotope from 292 – 278 cm, varying from 3.38 to 3.35 ‰. There is also a decrease in $\delta^{13}C$ in the same interval, 0.34 – 0.09 ‰.

Foraminiferal test fragmentation

Very low values of fragmentation were detected in H4, an average of 39.71 %. This interval starts with a sudden decrease in the value of foraminiferal test fragmentation.

Foraminifera

The stadial interval has both a high concentration of planktic foraminifera (1099.31 Foraminifera/g), and a high P:B ratio (4.21). The most common benthic foraminiferal species, *C. neoteretis* (42.89 %), increases throughout the interval. *E. excavatum* (15.16 %) is also quite common, however, its values decrease through out the interval. *C. reniforme* (13.37 %) has an abrupt peak, *M. barleeanus* (3.01 %) has a low value same as *C. lobatulus/A. gallowayi* (4.76 %), but they have a small abrupt peak in the middle of the interval. *E. vitrea* has a very low value in this interval of 1.03 %.

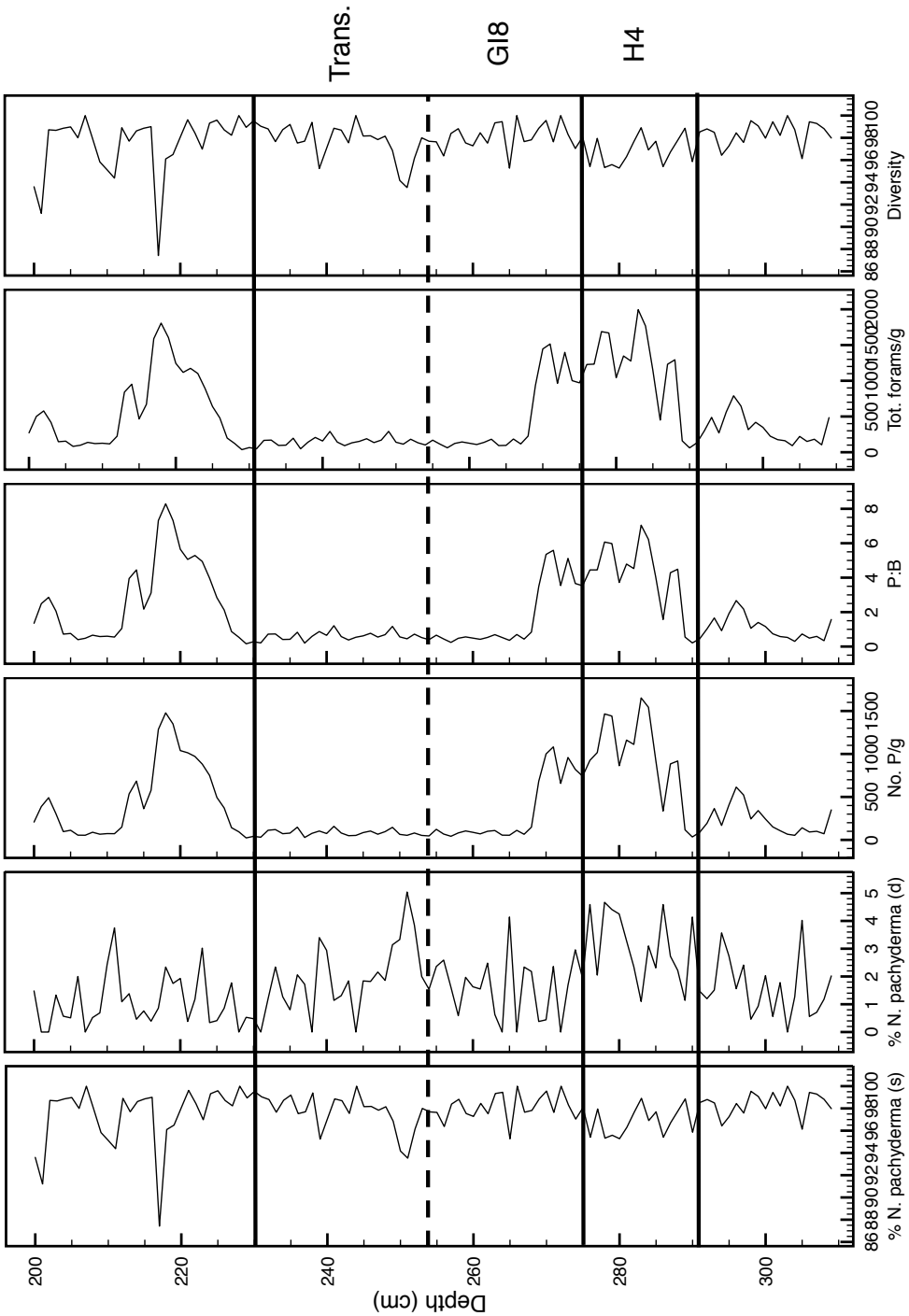

Figure 14 Foraminiferal data from core JM11-FI-15GC. H4 corresponds to Heinrich event 4. The GI8 is divided into two intervals separated by the dotted line. Trans. stands for transitional cooling interval.

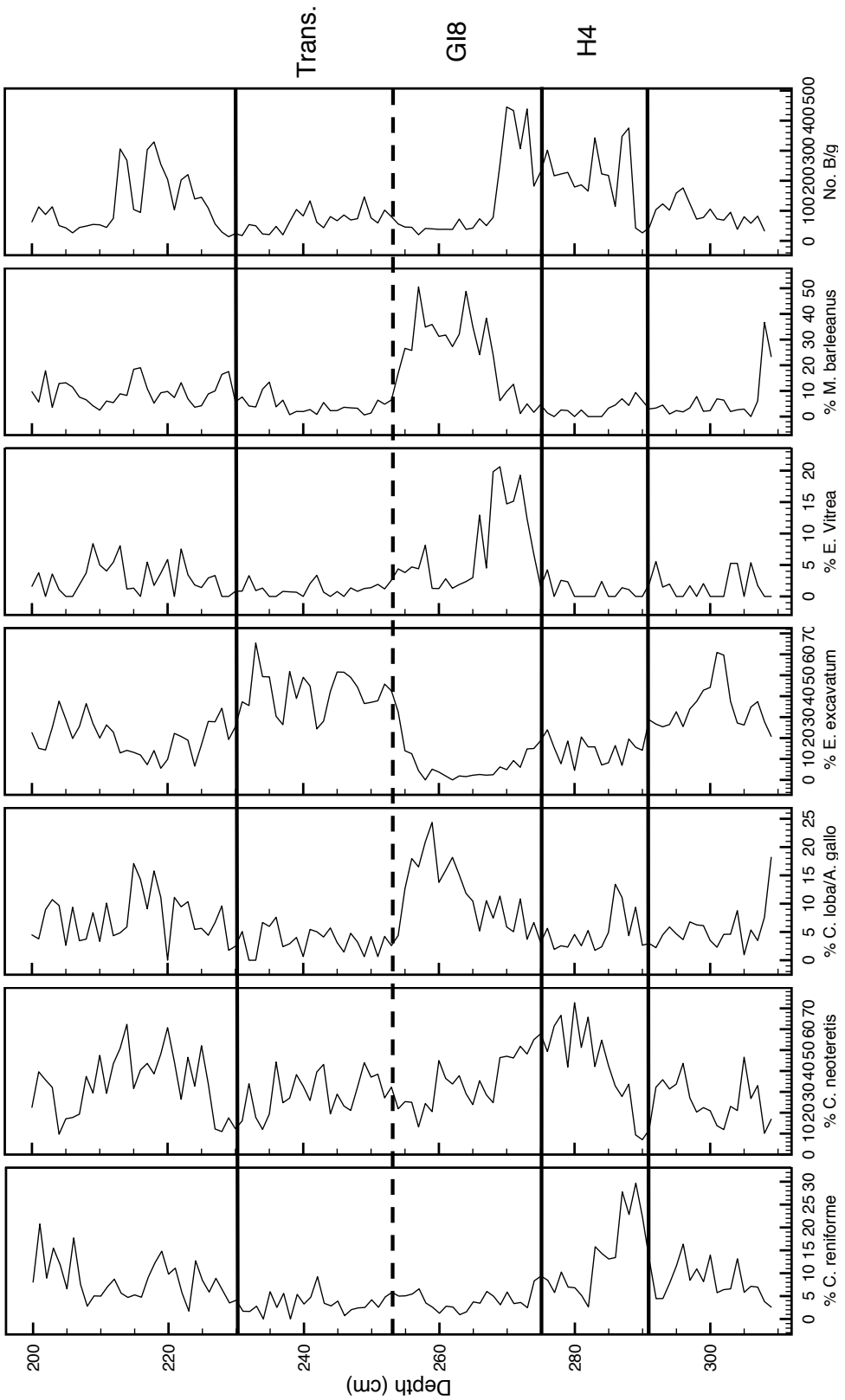

Figure 15. Distribution patterns of benthic foraminifera (in %) and concentration of benthic foraminifera (No. per gram dry weight sediment). The intervals are divided as in figure 12.

4.4 Tephra

The counted tephra was separated into two different groups; first light porous particles (porous tephra), possibly carried by the wind, and second the heavier, solid particles (blocky tephra), more likely to be carried by oceanic currents or ice rafted. As most of the samples contained some tephra, it was usually a background noise. The tephra that was found was very dark brown, almost black, and most likely of Icelandic origin; this could be confirmed by geochemical analysis. Porous tephra (Figure 16) shows two very distinct and sudden peaks. The highest peak is at 271 cm and the second lower one is at 260 cm. There is small peak at 220 cm.

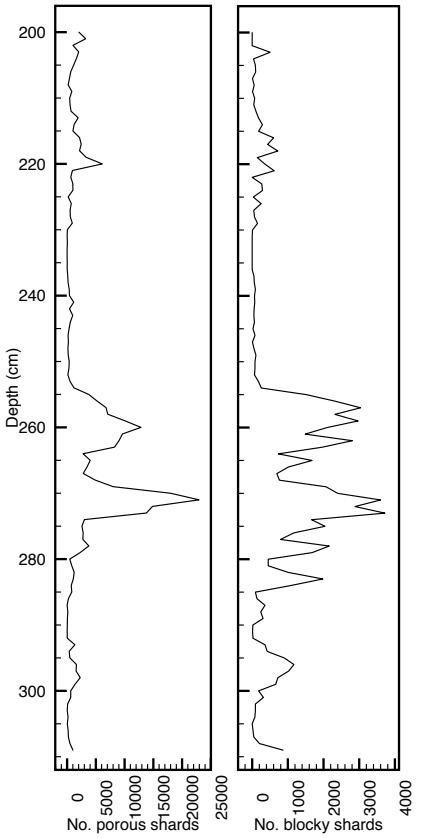

Figure 16 FMAZ-III has two distinct peaks both in porous and blocky tephra shards. Porous shards are the most abundant.

Figure 16 is quite different for the heavier tephra, as the peaks are not as well defined. Rather than having sharp peaks, it consists of smaller oscillations towards a high peak.

5 Chronology and construction of the age model

5.1 Chronology

Five samples were AMS-^{14}C dated. The ^{14}C ages were calibrated to calendar years based on the Fairbanks et al. (2005) calibration program (http://radiocarbon.ldeo.columbia.edu/research/radcarbcal.htm), as ^{14}C age is not same as calendar years (Table 1). A standard reservoir age of 400 years was subtracted before calibration. The North Atlantic has the average age of around 400-500 years in reservoir age, but in glacial time this reservoir age could have been far greater (Bard, 1988).

Table 1 Using 1 σ or 68 % chances that the correct age being within the curve. Abbreviation: NPS = N. pachyderma *(s). UBA No is the lab code of ^{14}Chrono Centre, Queen's University Belfast.*

UBA No	Dated material	Depth (cm)	^{14}C age	Error ±	Mean Calibrated years BP	Error ±	Remarks
28758	*NPS*	202	30,109	204	35,128	239	Near the top of core
28375	*NPS*	218	29,734	257	34,754	293	Peak in tot. forams
28376	*NPS*	271	33,771	416	38,76	432	Peak of tephra
28377	*NPS*	283	34,974	427	39,934	449	Sudden cooling
28759	*NPS*	309	37,463	476	42,189	447	Bottom of core

The sample from 202 cm was dated older than the one from 218 cm (see Table 2), therefore one of them had to be discarded. 202 cm was discarded, as it is common to discard the higher age as older material could be reworked into the sediment. When looking at Fairbanks et al. (2005) coral calibration curve, there is indication of a plateau between 28,000 and 30,000 ^{14}C age. That might also be the reason for the age reversal.

5.2 Sedimentation rate

By assuming constant sedimentation between radiocarbon dates, it is possible to estimate the sedimentation rate. By using an interval between two radiocarbon dates,

and the interval of depth that these radiocarbon dates were found, the rate can be calculated, as seen in Figure 17.

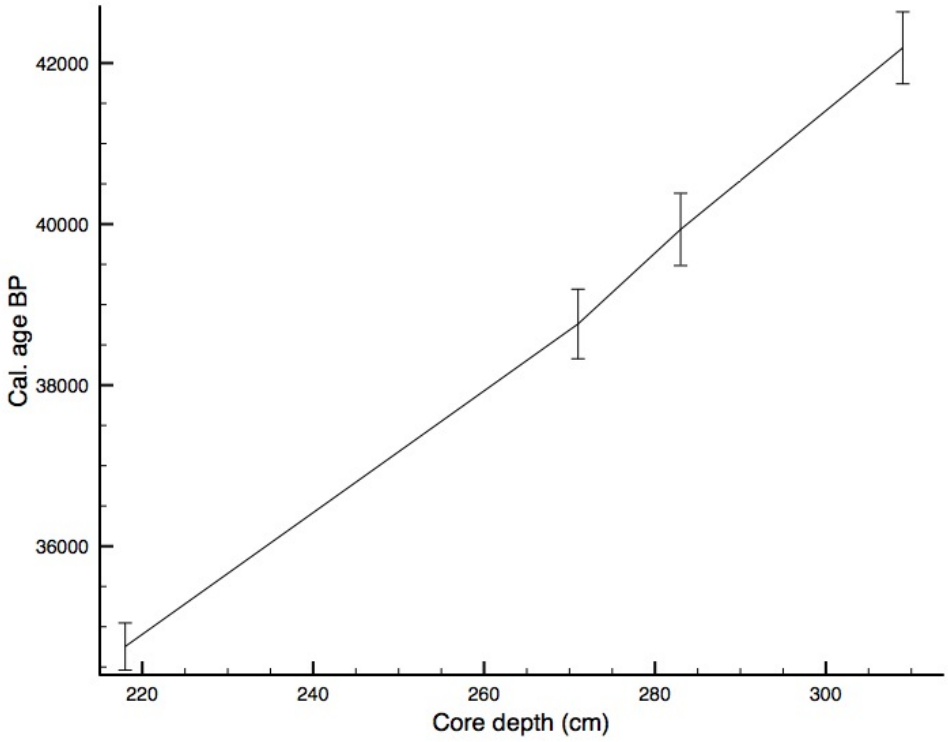

Figure 17 The sedimentation rate as function of core depth in cm. The error bar shown on the graph show the 1σ deviation for each of the calibrated age

Table 2 shows the average sedimentation rate between the calibrated ages. The sedimentation rate fluctuates from 8.41 – 45.94 cm/kyr.

Table 2 The average sedimentation rate between radiocarbon dates

Depth A (cm)	Depth B (cm)	Cal. years BP A	Cal. years BP B	Sedimentation rate cm/kyr
218	271	34,754	38,760	12.90
271	283	38,760	39,934	8.41
283	309	39,934	42,189	45.94

5.3 Correlation with NGRIP and construction of the age model

Here the JM11-FI-15GC data is correlated with the precise NGRIP data, and for that purpose planktonic foraminifera, calibrated ages, magnetic susceptibility and tephra

horizons were used. Four points were used, GI7, GI8, FMAZ-III and the sudden cooling in the beginning of H4, since these events should be found in both cores.

$\delta^{18}O$ values from *N. pachyderma* (s) correlated with the abrupt changes in the D-O event seen in the NGRIP core. *N. pachyderma* (s) is a planktonic species that reflects the sea surface temperature. The magnetic susceptibility is used for correlation as that during Heinrich events, there is a very low magnetic susceptibility and during interstadials the value is much higher.

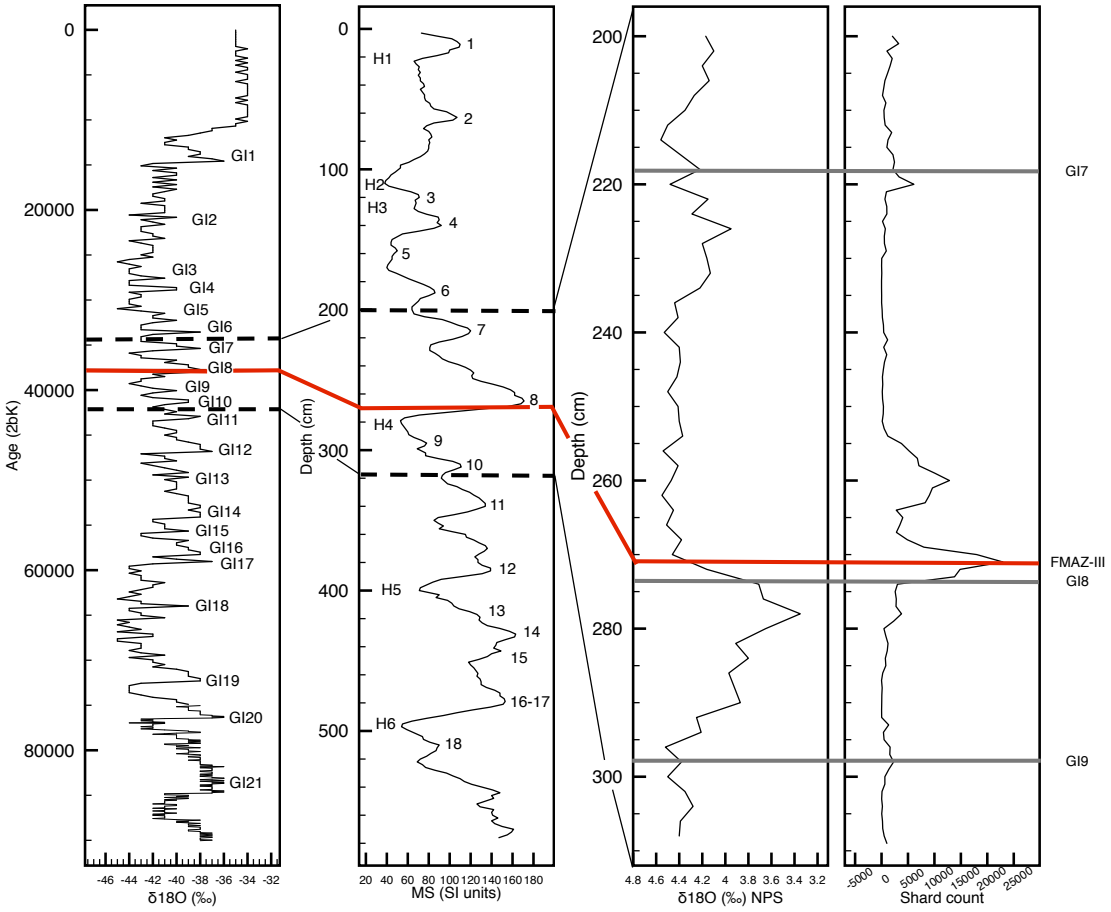

Figure 18 shows the NGRIP data (GICC05) compared to data from JM11-FI-15GC. The magnetic susceptibility is for the whole core and the investigated interval is within the dotted lines. The position of the interstadials is approximated based on results from Rasmussen et al. (2003). The interstadials that fall within the investigated interval are marked by gray lines. The red line is peak of the FMAZ-III tephra.

The depths for GI7 and GI8 were estimated by using the sudden increase in magnetic susceptibility and the sudden decrease in planktonic foraminifera. The FMAZ-III tie point was chosen from the largest peak found with the tephra shard count. The

sudden cooling is the beginning of H4 and it was estimated from the abrupt change in $\delta^{18}O$ that occurred both in the NGRIP ice core and in JM11-FI-15GC. The tephra layer FMAZ-III has a strong signal in the JM11-FI-15GC and is also found within the NGRIP ice core.

Looking at the data in Table 3 there is a large difference in the NGRIP and calibration age raging from -726 to 1694 years, but within the margin of error. Due to the reservoir effect, it seems logical that the difference in age should be a positive number and not negative as found for 218 cm. This could be the result of a possible plateau on the calibration curve. The cooling event has the largest age difference and shows similar what Olsen et al. (2014) noted, that stadial have much higher reservoir age than interstadials.

Table 3 shows the difference in ages between NGRIP and cal. years BP. NGRIP age (before 2000 years) is from Svensson et al., 2008.

Event	Core Depth (cm)	Cal. years BP	NGRIP age (b2k)	Difference (years)
GI7	218	34,754±293	35,480±661	-726
FMAZ-III	271	38,760±432	38,122±723	638
GI8	274	39,054	38,220±725	834
Sudden cooling	283	39,934±449	38,240	1694

Olsen et al. (2014) estimate that the reservoir age can be as high as 2000 years for H4. The reservoir ages before and after the Heinrich event seem to be lower. The reservoir age variations are associated with the changes in strength of the North Atlantic Drift. When it is a strong and there is deep convection the reservoir age is less than during times when it is weak (Olsen et al., 2014).

6 Discussion

Interpretation of the paleoenvironmental conditions

The data (shown in the previous chapter) will be interpreted in terms of oceanographic and climatic changes that occurred during the last glacial. The three larger interstadial, stadial and transitional cooling intervals are well defined and all the other smaller events in the record seem to follow the general trend.

6.1 Interstadial interval ~ 39,054 – 37,475 cal. years BP

Grain size distribution

The interstadials shows an increase in the % of the grain-size 63 – 100 µm from the beginning of the interval. When comparing the % of 63 – 250 µm to the stadial, it becomes clear that sediments during the stadial intervals were finer than the interstadials sediments, consisting of clays with IRD (Figure 11). The concentration of IRD (no/g) is still high in the beginning of the interstadial interval, but decreasing. This decrease in IRD through the interval can be understood as either that the icebergs contained less IRD or, more likely, there were fewer icebergs due to warmer surface waters. There is an indication of warmer conditions, the increase of planktonic foraminifera, which prefer warmer waters such as *N. pachyderma* (d) and *G. quinqueloba* (e.g. Fronval et al., 1995; Rasmussen et al., 1996a;b). Higher $\delta^{18}O$ values indicate less melt water from icebergs in the interstadials, as seen in other nearby marine records (Fronval et al., 1995; Rasmussen et al., 1996).

The water content also increases, indicating a greater spacing in the grains (higher porosity). Not only is there a change in the grain size distribution (see Table 2) but there is an indication of higher sedimentation rates during the interstadials. As observed by Rasmussen et al. (1996, 1998) the sediments at interstadial times are different from stadial sediments as there is an increase in the content of silty, basaltic sediments and higher proportions of smectite. This was also observed in the North Atlantic by Kissel et al. (1999) and Moros et al. (2002). It is most likely that the sediment in JM11-FI-15GC is of the same origin.

Multi-Sensor Core Logger data

MS (Figure 10) changes abruptly to higher levels in the beginning of the interstadial intervals. When MS is compared to the $\delta^{18}O$ values (Figure 10) there is a clear indication that, when $\delta^{18}O$ value rises to higher values, so does MS. In this study the sediments were not divided into groups according to their origin, however, that was previously done by Rasmussen et al. (1998), their data indicated that MS is mainly controlled by the concentration of basaltic particles and smectite. The concentrations are high in the interstadial intervals, and were probably carried with the bottom currents from volcanic rich areas off Iceland. The data shows that similar oceanic circulation was present during the interstadials and present time (e.g. Rasmussen et al., 1996, 1998; Kissel et al., 1999). The wet bulk density is low during this interval, as the water content is high and there is little compaction of the sediments (Geotek, 2014).

Planktic $\delta^{18}O$ and $\delta^{13}C$ values

Fluctuations in the $\delta^{18}O$ values in *N. pachyderma* (s) can reflect changes in the global ice volume, local temperature, salinity (Mix and Ruddiman, 1982) and fresh water or melt water input (Maslin et al., 1995). According to Bauch et al. (1997) *N. pachyderma* (s) might not reflect surface water conditions, but rather the upper water masses, due to the average calcification depth is between 100 to 200 m.

In the beginning of the interstadial the $\delta^{18}O$ values abruptly increase (Figure 10). Implying that there is an increase of the heavier oxygen isotope ^{18}O within the foraminiferal tests, and that there is less inflow of melt water from icebergs indicating warmer climates (cf. Rasmussen et al., 1996). Looking at the same interval for $\delta^{13}C$, there is a sudden increase in these values. The $\delta^{13}C$ values are used for tracking changes in both the circulation and nutrients in the ocean (Kroopnick, 1985). During the Pleistocene there is a shift in the $\delta^{13}C$ ratio of 0.3 between the glacial and interglacial due to changes in the terrestrial reservoir (Linsley and Dunbar, 1994). The increase in $\delta^{13}C$ values in core JM11-FI-15GC is related to millennial scale oceanographic changes and that is in itself probably related to better ventilation in the subsurface water mass and less sea-ice at the surface (Zamelczyk et al., 2012).

Foraminiferal test fragmentation

During the interstadial there is a high degree of fragmentation. This increase in fragmentation is taken as an indication of dissolution of calcium carbonate ($CaCO_3$) (Le and Shackleton, 1992). The amount of $CaCO_3$ within the sediment is related in part to biological productivity, which again is strongly related to environmental conditions such as temperature, nutrients and sea-ice cover (Le and Shackleton, 1992; Hebbeln et al., 1998; Zamelczyk et al., 2012).

During the interstadial interval there is indication of stronger dissolution relative to the stadial interval, and affecting the planktonic foraminifera more (Figure 14). This is shown by a decrease in concentration of foraminifera and also in the lowering of the P:B ratio relative to stadial intervals. After a planktonic foraminifera dies its test descends through the water column, which is affected by dissolution as it sinks. The dissolution can also occur at the sea floor and after burial in the sediment (Steinsund and Hald, 1994; Zamelczyk et al., 2013). The dissolution is controlled by a number of factors; the amount of dissolved CO_2 in the water (and hence organic productivity), temperature, salinity and depth (Steinsund and Hald, 1994; Hald and Steinsund, 1996).

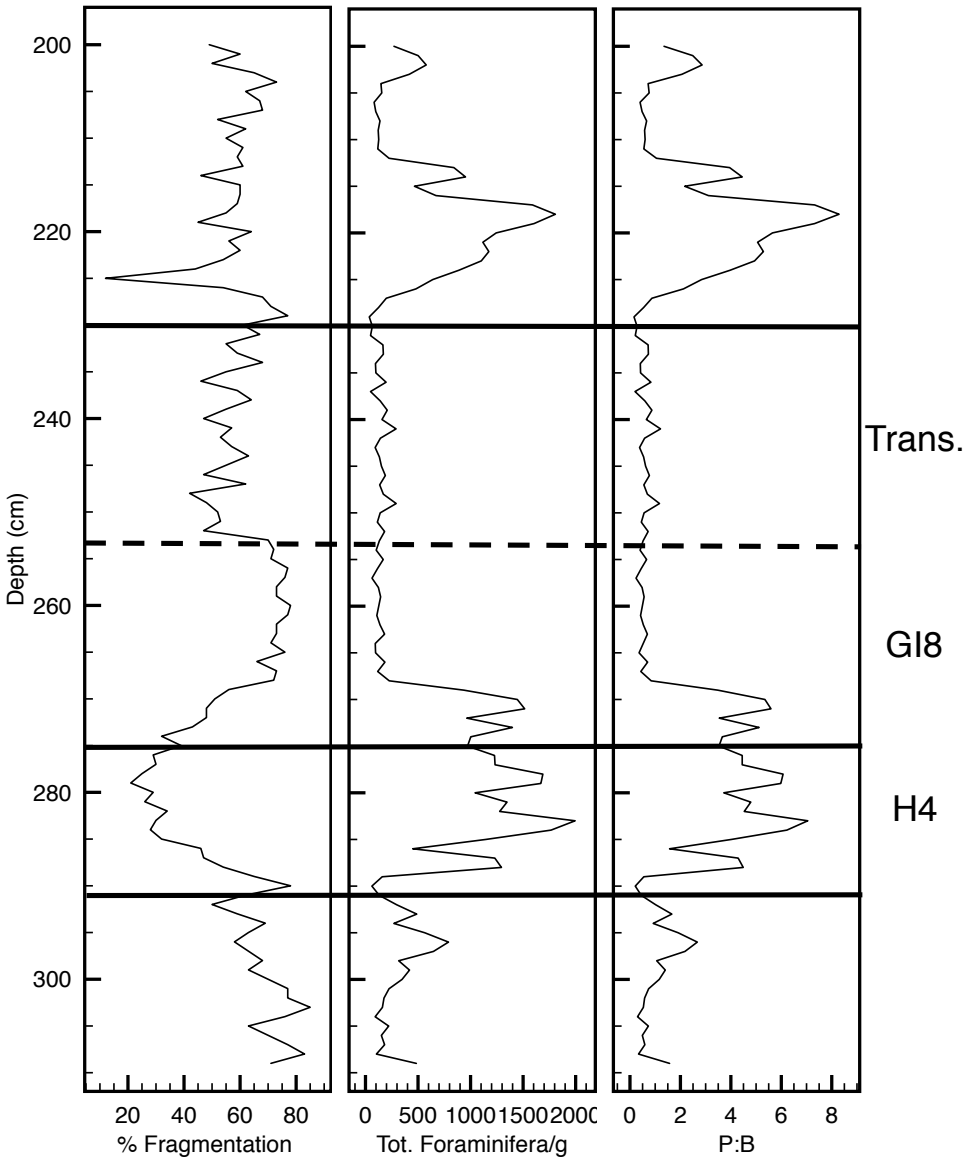

Figure 19 The % of fragmentation compared to concentration of foraminifera and the ratio between planktonic and benthic foraminifera.

This increased dissolution is likely to be caused by increased surface productivity (Rasmussen et al., 2002a; Zamelzcyk et al., 2012) during the interstadial. Increased organic matter can lower the pH in the bottom sediments, which increases carbonate solubility (Scott et al., 2008). High dissolution during the interstadials might have caused a large error in the data, as planktonic foraminifera that indicate warmer sea surface temperature were very few in the investigated interval (see all planktonic foraminifera in Appendix Figure 25). Some species are more vulnerable against

dissolution (Berger, 1971), which causes them to be underrepresented in the samples from interstadial intervals. *T. quinqueloba,* for example is especially sensitive to dissolution (Zamelczyk et al., 2012) and this species is associated with warm and saline Atlantic Water (Jennings et al., 2004).

Foraminifera

In this interval *N. pachyderma* (d) reaches its highest relative abundance (Figure 14), over 5.00 %, which indicates stronger influence of relatively warm water (subpolar water) (Kellogg, 1980). At the same time there is an increase in "other" species (*G. bullodies, G. glutinata, G. uvula and T. quinquloba).* These are all subpolar species associated with warm and saline Atlantic water (Bé and Tolderlund, 1971; Jennings et al., 2004). Although, all these species combined make up only 2.50 %, their presence indicate an inflow of warm Atlantic Water. Other studies done in the region show a much higher level of warm water indicating planktonic species in GI8 (e.g. Rasmussen et al., 1996b).

One of the most interesting peaks in the relative abundance of benthic foraminiferal species during the interstadial belongs to the species *M. barleeanus* (Figure 15). This is an adaptable species, but is very dependent on organic material as a food supply (Caralp, 1989), which can indicate higher productivity. Rasmussen et al. (1996b) indicated that this distribution of *M. barleeanus* is a sign of similar bottom water conditions as today with deep convection. Just before this abrupt peak, there is a smaller peak in percentage of the benthic foraminifera *E. vitrea.* This species is connected to an increasing influence of organic matter (Ernst et al., 2005), similar to *M. barleeanus,* however, this species is also tolerant of low oxygen levels and is considered to be an opportunist (Gustafson and Nordberg, 2001). This might indicate that the interval starts with a strong influence of organic matter, but that the food supply was still unstable, which could lead to temporal anoxia (Rasmussen et al., 1996b). When conditions got more stable then *M. barleeanus* quickly colonized the area.

There are also strong bottom currents in the interstadial as seen by higher relative abundance of the two bottom current indicator species *C. lobatulus* and *A. gallowayi* (Hald and Steinsund, 1996) (Figure 15).

6.2 Transitional cooling interval ~ 37,399 – 35,661 cal. years BP

Grain size distribution

The data from the grain size distribution predominantly shows an increase in the concentration of IRD from the interstadial (Figure 10). The value is not as high as for the stadial, but it indicates an increase in material transported by icebergs. The peaks are not as stable as for the stadial interval, which could indicate fluctuations in the temperature of the surface waters.

Multi-Sensor Core Logger data

The magnetic values are declining in this interval, reflecting reduction in bottom current strength (Rasmussen et al., 1996b).

Planktic $\delta^{18}O$ and $\delta^{13}C$ values

This interval is mostly in-between the values, recorded in stadials and interstadials.

Foraminiferal test fragmentation

The fragmentation does not show as high peaks as in the interstadial (Figure 19), which could be interpreted as an improvement in preservation and decreasing surface productivity. There was a very low concentration of foraminifera (148.21 Foraminifera/g), this value was even lower than for the interstadials (Figure 19). The cause might be that there is more dissolution than during the interstadials, such that even fragments have been dissolved or were of so poor quality as not to survive the sieving process. In any case, the low number of foraminifera would indicate very harsh environmental conditions.

Foraminifera

The dominating benthic foraminiferal species in the transitional cooling interval is *E. excavatum* (Figure 15). Its high values suggest fluctuating bottom conditions with a reduced vertical circulation (Rasmussen et al., 1996b). This could be an indication of an unstable cold environment, which is difficult for other species of foraminifera to thrive in. *E. excavatum* can quickly colonize environments that are hostile to other foraminifera (Steinsund et al., 1994). There is a reduction in bottom currents as seen by decreasing

relative abundances of *C. lobatulus* and *A. gallowayi.* There is also indication of reduction in the deposition of organic material as seen by decreased percentages of *M. barleeanus.*

6.3 Stadial interval ~ 40,628 – 39,151 cal. years BP

Grain size distribution

The interval starts with very high percentage of the grain size fraction 63 – 100 µm (Figure 11). This is also seen in the low water content, which indicates low porosity. Thereafter the content of the coarser sediment increases, especially the concentration of IRD rises. This increase in coarser fractions is most likely caused by an increase in ice rafted material.

Not only is there an indication of increased iceberg activity in the area, but there is also a sudden change in color to a light gray color (Figure 13) seen in H4. Rasmussen et al. (1998) also noticed this color change within their core records from the Faeroe Islands Margin and explained it by a change in the origin of the sediments. The gray sediment has a high percentage of $CaCO_3$ and quartz grains and resembles sediments from the Shetland-Scotland Shelf. The data also suggests a decreased sedimentation rate during the stadials, as less material is transported to the area by bottom currents.

Multi-Sensor Core Logger data

The MS is very low during the stadial interval (Figure 10), which reflects the changes in the sediment composition (Rasmussen et al., 1998). The measured density is higher, indicating more compact sediment. This density change fits with the decrease in water content (Figure 11).

Planktic $\delta^{18}O$ and $\delta^{13}C$ values

In the interval of interest, 40,628 – 39,151 cal. years BP, there is a large drop in the $\delta^{18}O$ values (Figure 10). The period is correlated to H4 and it is unlikely that this drop is caused by increased warmth in the sea surface, as Heinrich events occur at a time of extreme cooling as seen in ice cores and marine cores from the North Atlantic (Bond et al., 1993). The change is rather a cause of decreased salinity due to an inflow of melt water. This is supported by Maslin et al. (1995), as they found that sea surface salinity decreased during Heinrich events and especially during H4. The sea surface

temperature was also lower, which could have been caused by freezing surface water (Maslin et al., 1995). The $\delta^{18}O$ values indicate therefore a time of large influx of melt water, which caused the fluctuations in the $\delta^{18}O$ values, as icebergs have very low $\delta^{18}O$ values (Roche et al., 2004). This is supported by the increased IRD concentration through this interval indicating that the melt water arrived from the icebergs. $\delta^{13}C$ experiences also lower values during stadials (Figure 12), which indicates weaker deep-water formation and less ventilation (Vidal et al., 1997) because of stratification of the surface (Peck et al., 2007).

Foraminiferal test fragmentation

According to data presented in this thesis there is less fragmentation and less dissolution of foraminiferal shells during stadials (Figure 19). In general, there is better preservation of foraminifera during colder periods. This could be further confirmed by using average test weight. The preservation of $CaCO_3$ during colder climate could be caused by less organic production due to more sea ice cover (Scott et al., 2008; Zamelczyk et al., 2012). During this interval there is increase in concentration of foraminifera and much higher P:B ratios. Planktonic foraminifera seem to have finer tests and presence of juveniles, probably because of better preservation in the stadial interval.

Foraminifera

The planktonic foraminifera show quite interesting values in the stadial interval. *N. pacyderma* (d) is more abundant during stadial (2.96 %) than interstadial (1.59 %) intervals. The *N. pachyderma* (d) shows similar values as Rasmussen et al. (1996b) in the stadials, but has much lower values in the interstadial as in their data it reaches up to 9 % in GI8. Their data points towards colder surface water temperature in the stadials (Rasmussen et al., 1996b), not opposite as the data shown here (Figure 14). This polarity is possibly connected to stronger dissolution during interstadials.

Benthic foraminifera are dominated by *C. neoteretis*, with values up to 72 %. This is an arctic species that indicates the presence of the Atlantic Intermediate Water in the Nordic Seas. It thrives in cold bottom waters (Jennings and Helgadóttir, 1994). *C. neoteretis* is often found with the "Atlantic" group as described by Rasmussen et al. (1996b). *C. reniforme* as an abrupt peak in the start of the interval, this species also

prefers low temperatures and is as well an indicator of Atlantic Intermediate Water (Jennings and Helgadóttir, 1994). Both of the species prefer fine grained muds as substrates (Mudie et al., 1984; Mackensen and Hald, 1988; Steinsund et al., 1994).

There is an indication of stronger bottom currents in the beginning of the interval, as seen by a small peak in percent of *C. lobatulus* and *A. gallowayi*. This peak occurs at same time as there is an increase in % *C. reniforme,* it is possible that *C. reniforme* also responds to increase in bottom currents. The investigation would benefit from sortable silt data, for further investigation into the changes in bottom currents.

7 Comparison to other studies

This is a high-resolution study of selected Dansgaard-Oeschger events dating around Heinrich event 4 and Greenland interstadial 8, comprising the time interval 40,628 – 35,661 cal. years BP. The interval investigated spans from Greenland interstadial 10 to Greenland stadial 7, comprising the time interval 42,102 – 33,393 cal. years BP. This chapter is about comparing the data that was interpreted in the previous chapter with other studies from the region of the Nordic Seas and the North Atlantic.

7.1 Environment and climate

The last glacial period (~120,000 – 10,000 years BP (Rahmstorf, 2003)) was characterized by abrupt climate and environmental changes. These changes can be seen within the marine realm, in terrestrial records and within glacial ice. Large ice sheets, such as the Greenland ice sheet, can have a large effect on the climate due to their enormous size (Clark et al., 1999). The North Atlantic Ocean (above 40°N) has been influenced by the North American ice sheet in the past, when cold wind blows over the ice sheets it can cool the surface waters by 10 °C or more (Ruddiman et al., 1986). They can cause climate changes due to ice-albedo and radiation balance. Their sizes can also influence the wind patterns and sea level changes (Clark et al., 1999).

There was increase of glacial icebergs in the North Atlantic Ocean and Nordic Seas every 2000 to 3000 years during the last glacial period, as indicated by increase in the deposition of IRD. There is an increase in sea surface cooling before these events take place. These correspond to the D-O events, which indicate a close link between the temperature above Greenland and these smaller ice-rafting events. The events are most likely caused by climate change as they contain both material from the Greenland and the Icelandic ice cap, and from the Hudson Strait and Gulf of St. Lawrence, which then calved at similar time. The events, where the Laurentide ice sheet contributes with icebergs and IRD, are termed Heinrich events, which occur every 7000-10,000 years BP (Bond and Lotti, 1995). The Heinrich events last longer and are always followed by a larger and longer-lasting interstadial interval (Bond et al., 1993) (Figure 20).

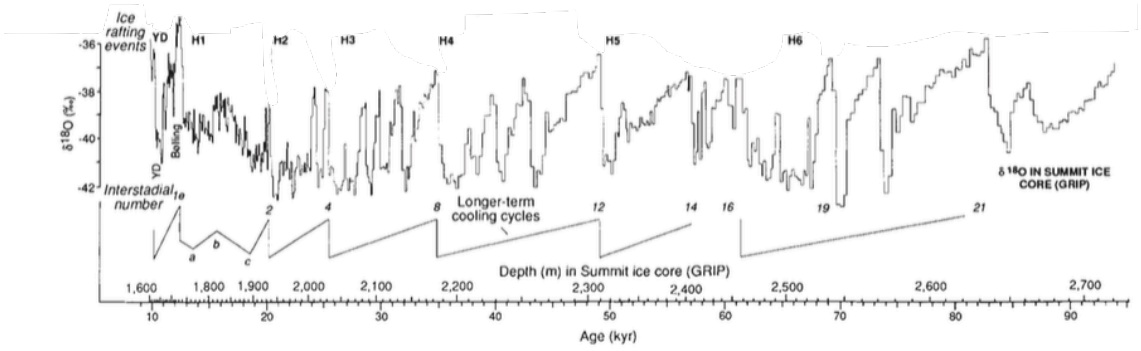

Figure 20 The $\delta^{18}O$ values are from GRIP ice-core from Greenland. The cooling cycles end abruptly with an ice rafting event termed Heinrich event (marked by H) (modified figure from Bond et al., 1993).

During the D-O events it is estimated that the temperature over the Greenland ice-sheet fluctuated by some 15 °C. The temperature at the last glaciation sometimes reached more than 20 °C lower than today (maxing at 25 °C lower) (Johnsen et al., 2001).

The Milankovitch theory is based on external mechanisms as causes of climate change (Maslin et al., 2001). According to the Milankovitch theory of climatic forcing the ice-volume is dominated by 100,000, 41,000 and 21,000 years cycles. These cycles correspond to eccentricity or orbital configuration, obliquity or the tilt of the earth and precession. These cycles effect the insolation on the earth and therefore can influence climate. The 100,000 year cycle dominates the later part of the Pleistocene (last 900,000 years BP), and it corresponds to extreme glacial intervals (Pisias and Moore, 1981). Before 900,000 years BP, the interglacial and glacial cycles followed the 41,000 cycles. The cause of this change from 41,000 to 100,000 year-cycles is not understood (Maslin et al., 2001).

The Milankovitch theory cannot however, fully explain the changes that occurred during the late Pleistocene, as the changes happened on millennial scale (much shorter and too frequent). Some scientists believe that the ice sheets may be the cause of the millennial scale abrupt changes (Clark et al., 1999). However, the causes of these events are still debated even though their presence has been known for decades (Bond et al., 1999).

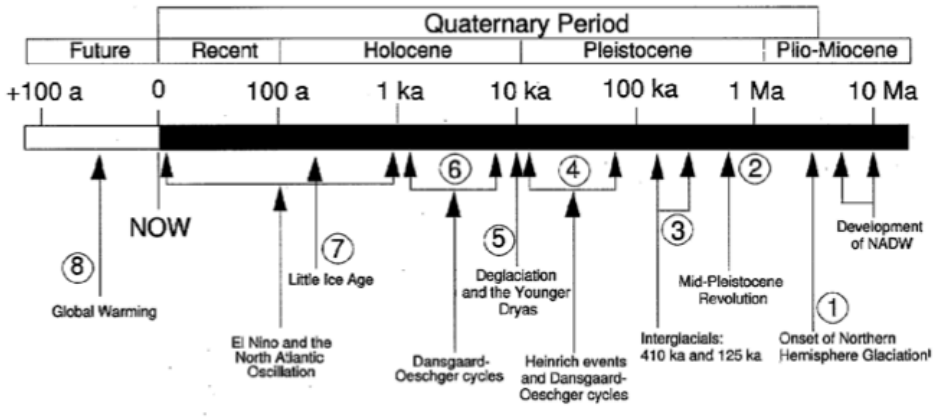

Figure 21 The figure shows that the Northern hemisphere glaciations started in Miocene-Pliocene. The change from 41,000 to 100,000 glacial-interglacial cycles is seen in the figure. This change in cyclicity must have been internally forced (figure from Maslin et al., 2001) The little ice age is thought to be connected to the millennial scale cycles that are behind D-O events according to Bond et al. (1999).

Bond et al. (1999) argue that D-O events are caused by 1000 to 2000 climate rhythms, rather than by ice sheet instabilities. The climatic changes are result of these short cycles that can be seen in data spanning 80,000 years. Also, they indicate that the D-O events are just an amplification of these cycles. These cycles are forced by a mechanism that is independent of glacial and interglacial climates, as these are also found within sediments from the Holocene (Bond et al., 1997). Rahmstorf (2003) argues that these cycles are too precise to have been caused by the Earth system, rather that they have their origin outside of the Earth. However the mechanism behind them is still unknown.

7.2 Paleoceanography in the vicinity of the Faeroe-Shetland Channel

JM11-FI-15GC is taken from the Fugløy Ridge in the western part of the Faeroe-Shetland Channel, which is an important area of water exchange between the Atlantic Ocean and Nordic Seas (Hansen and Østerhus, 2000). The last glacial period is characterized by abrupt changes, which can occur even within a few decades or less (Dansgaard et al., 1993). These changes are not only seen in the Greenland ice cores, but also within the marine realm.

The Holocene is considered to be a fairly stable period compared to the Weichselian glacial. The glacial period is characterized by abrupt climate changes, stadial and interstadial intervals. The interstadials are believed to have similar oceanic circulation as today, with convection in the open sea and formation of deep water

(Rasmussen et al., 2002a). However, during stadials the circulation was greatly reduced, as was the formation of the NADW. There was less influence of warm Atlantic Surface Water, and the surface waters became much colder during the stadials (Broecker et al., 1990). The convection is thought to have stopped or greatly reduced in stadials because of freshening of the sea surface (Rasmussen et al., 1996) due to increasing number of icebergs. This increase in icebergs is seen in the data from JM11-FI-15GC by increase in concentration of IRD and also in low $\delta^{18}O$ values (Figure 10). Lower values of $\delta^{13}C$ (Figure 12) indicate at the same time stratification of the surface (Peck et al., 2007).

The planktonic foraminifera in core JM11-FI-15GC do not show this change towards cooler climate, as discussed in the interpretation this might be caused by dissolution during interstadials, which could obscure the values. When there is cooling, both shown in the NGRIP ice cores (change in $\delta^{18}O$) and other cores in the vicinity of JM11-FI-15GC, it is unlikely that there is warming in sea surface temperature (SST) in H4 (according to the data there is more of *N. pachyderma* (d) in stadial than in interstadials intervals (Figure 25 in Appendix)). Especially as other studies (Cayre et al., 1999; Paterne et al., 1999; Sánchez Goñi et al., 2000) do not indicate increased SST at H4, on the contrary they show decrease. There is also another issue to keep in mind when using percent of *N. pachyderma,* since generally there is 1-3 % right coiling forms that genetically belong to the left coiling species (Darling et al., 2006). The selective dissolution in the interstadials is most likely caused by increase in surface productivity of organic material.

7.2.1 Bottom conditions

The changes that occurred during the last glacial period are not confined to the upper sea surface layers as the formation of cold deep water in the Nordic Seas and the NADW has large influence on the bottom conditions as well. The change in the bottom fauna is quite abrupt and the interstadials, transitional cooling and stadial intervals can be clearly seen.

The bottom currents at interstadials are similar as today with formation of NADW, this is indicated by high abundance of *M. barleeanus* (Rasmussen et al., 1996b). The magnetic susceptibility is high (Figure 10), which is due to presence of basaltic material from volcanic rich areas (Rasmussen et al., 1998). This transport occurs when

there is formation of NADW. This stronger convection is also seen in increased values of *C. lobatulus* and *A. gallowayi*. The formation of NADW is slowly decreasing in the transitional cooling interval (Figure 15).

The formation of the NADW is greatly reduced or stopped during the stadials (MacManus et al., 2004). This is shown in the decrease in magnetic susceptibility. During the H4 event, there is a clear change in composition of the sediments, and a color change (Figure 13). The abundance of *C. neoteretis* (dominating species) and *C. reniforme* indicate the presence of the Atlantic Intermediate Water (Jennings and Helgadóttir, 1994). When the convection is reduced the Atlantic Intermediate water can enter into the Faeroe-Shetland Channel (Rasmussen et al., 1996b). This water flowed under the cold and light surface water and warmed up the deep-water masses (Rasmussen and Thomsen, 2004; Marcott et al., 2011, Ezat et al., 2014). The water is most likely stratified as indicated by the $\delta^{13}C$ values. Cores from the vicinity of JM11-FI-15GC, show a group termed as "Atlantic species" (Rasmussen et al., 1996a;b; Rasmussen and Thomsen, 2004). These species are mostly found in waters with temperature above 3.5 °C (Rasmussen and Thomsen, 2004). Their presence should be quite strong during H4, but however they could have been overlooked or put into the group "other"(unknown) when identifying to species level. As there is little dissolution seen in the core in the stadial intervals it is very improbable that dissolution is to blame for their absence.

During stadials there is lower sedimentation rate relative to the interstadials intervals. These cyclic sedimentations rates correspond to the D-O events. During times of stadial and interstadials there is a change in the oceanic circulation system. During the stadials the circulation is greatly reduced (Broecker et al., 1990), with relatively weaker currents with less transporting capacity (Rasmussen et al., 1998; Kissel et al., 1999; Moros et al., 2002).

Another indication of reduction or stopped production of NADW is indicated by increased reservoir age as seen in the H4 interval. The data in JM11-FI-15GC indicates higher reservoir age at H4 than at the start of the interstadials GI7 and GI8. Olsen et al. (2014) showed also these results in a core from the central part of the Faeroe-Shetland Channel, as when there is weak convection the reservoir age rises.

7.2.2 Theories regarding changes in circulation

The mechanism that 'turns-on' and 'turns-off' the convection and formation of NADW is not fully understood. Brocker et al. (1990) suggested that it has to do with changes in salinity. The idea is that the circulation stops due to decreased density caused by less salinity of the water. These are the periods of ice growth and increase in release of melt water from the ice. This is followed by a period of salt build up, when ocean circulation decreases and less heat is released to environment due to loss in circulation and less salt is exported from the system. Eventually enough salt causes renewal of convection that causes warming of the climate and surface inflow of warm Atlantic Water (Brocker et al., 1990).

Dokken and Jansen (1999) suggest that there was always formation of deep water, but it was formed by two different processes. The interstadials are times of normal open ocean convection, but in stadials it was driven by brine formation. They suggest that is the cause of the low $\delta^{18}O$ found in benthic foraminiferal tests. This brine formation in their opinion eventually restarted the convection, and eventually ends the stadials.

The data from JM11-FI-15GC argues against the theory from Dokken and Jansen (1999). During the stadials there was relative low fragmentation, high concentration of foraminifera and the ratio of P:B was also high (Figure 19). The data during stadials indicate that the foraminifera were well preserved (see above in 'Discussion' about fragmentation in stadials). If there was brine formation it would be more likely that the foraminifera would show high dissolution, as is seen during the interstadials. Brines are cold, dense waters, rich in CO_2 (Steinsund and Hald, 1994). Formation of brines transports CO_2 down the water column, and increase the acidity the water (Anderson et al., 2004), which would lead to increase in dissolution, not preservation as is seen in the data (Figure 19). In Storfjorden in Svalbard it has been shown that brine is corrosive to calcareous tests (Rasmussen and Thomsen, 2014). Therefore, it is unlikely that this theory explains the change in circulation from stadials to interstadials.

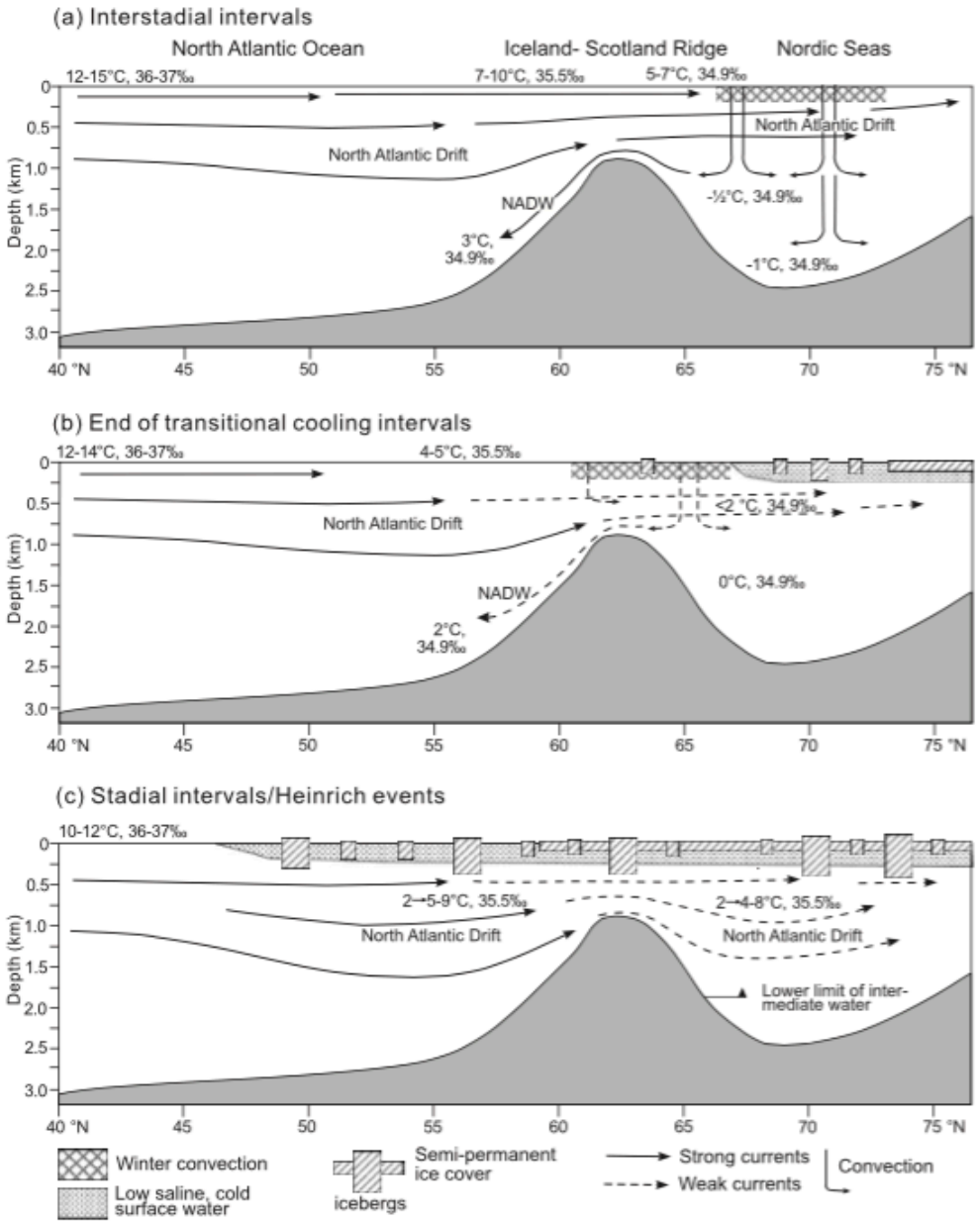

Figure 22 (a) Interstadials; show very similar convection as we might expect today (b) Transitional cooling intervals; there is indication of slowing formation of NADW (c) stadials/Heinrich; there is indication of Atlantic water flowing underneath the colder surface water, with reduced or no formation of NADW (figure from Rasmussen and Thomsen, 2004)

Rasmussen et al. (1996a;b) suggest rather that warm Atlantic water still flowed towards the Nordic Seas in the colder periods of the stadials, but this warmer water flowed underneath the lighter and colder surface water (Figure 22). The warmer water slowly warmed the intermediate water, causing decreased density. The change in density can have a great impact on the halocline. This could have caused the water column to become unstable and eventually could lead to it overturning. This process could be the reason for starting up the thermohaline convention in the Nordic Seas again

and explain the abrupt warming (Rasmussen and Thomsen, 2004). This theory is proving to be more likely, due to number of reasons. First, if there was brine formation that would lead to stronger dissolution of foraminifera during stadials. The results from core JM11-FI-15GC shows that the preservation during the stadials was the best of the entire studied record (Figure 19). In addition, *C. neoteretis* was very common during stadials (Figure 15) and today thrives at -1°C with salinity between 34.91 – 34.92 ‰ (Mackensen and Hald, 1988; Steinsund et al., 1994), but also in warmer Atlantic Water below a surface layer of cold polar water (Jennings and Helgadóttir, 1994). The water formed in brine formation would be very cold and of high salinity and corrosive, which would probably not be suitable conditions for *C. neoteretis.* The presence of this species suggests that there was warm Atlantic water beneath the colder surface waters (Rasmussen and Thomsen, 2004). A new article from 2014 by Ezat et al. demonstrate that there was most likely 2 – 5 °C increase in bottom water temperature during the stadials, and up to 6 °C in stadials connected to Heinrich events. Records from the North Atlantic show similar degrees of warming at the bottom for Heinrich events H6, H4 and H1 (Marcott et al., 2011). The new data presented here (Figure 19) thus supports that there was no (or negligible) brine overflow during stadials and Heinrich events.

7.2.3 Regional outlook

The Faeroe-Shetland Channel is a part of the Greenland-Scotland Ridge, which is intersected by number of deep channels. These channels are gateways for deep cold water to flow into the North Atlantic (Hohbein et al., 2012). The ridge separates the Arctic Mediterranean (the Nordic Seas and the Arctic Ocean) from the Atlantic Ocean. Most, or 90 % of all inflowing water to the Arctic Mediterranean is Atlantic in origin (Hansen et al., 2008). The Atlantic water flows mainly through the Icelandic-Faeroe Ridge and through the Faeroe-Shetland Channel (Orvik and Niller, 2002). This flow of warm waters through the ridge keeps the northern Atlantic on average 5 °C warmer than if it would be reduced or stopped (Broecker, 1991).

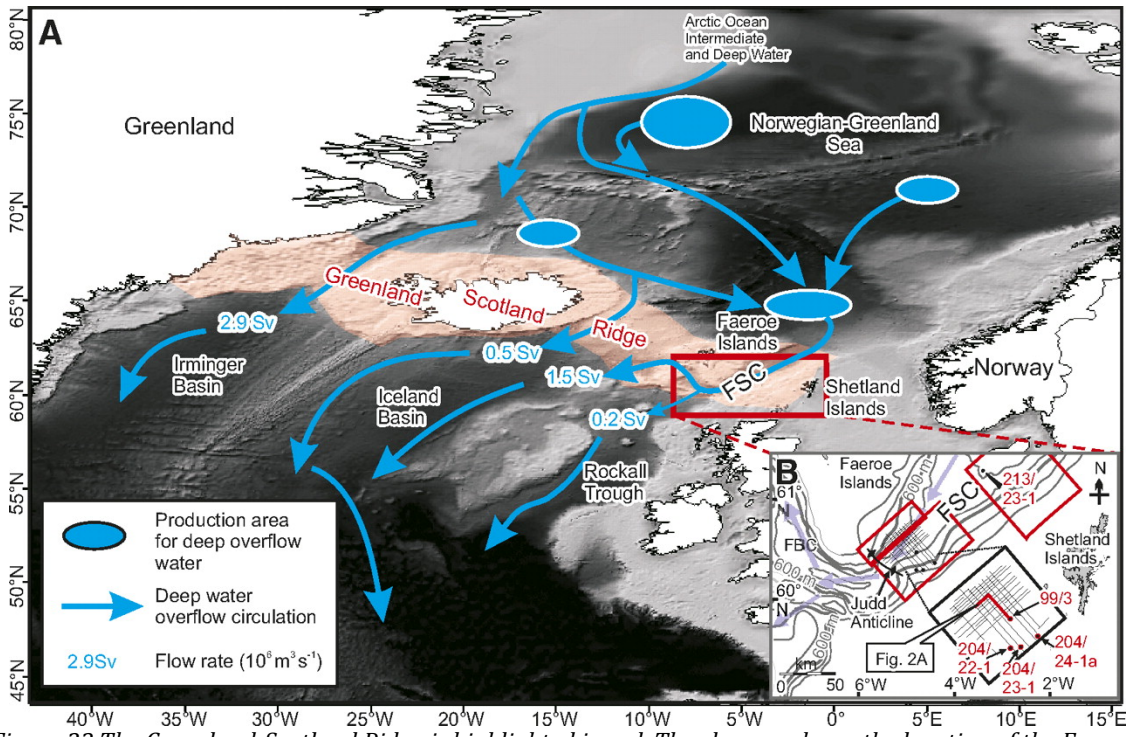

Figure 23 The Greenland-Scotland Ridge is highlighted in red. The close up shows the location of the Faeroe-Shetland Channel (FSC) and Faeroe Bank-Channel (FBC). This figure shows the main gateways for deep water overflow (Figure from Hohbein et al., 2012).

The formation of the NADW is very sensitive to a supply of large amounts of fresh water, which can have drastic effects on the strength of convection in the Nordic Seas. Reducing the strength can have drastic climatic effects over Greenland and northwestern Europe and cause drop in the air temperature of 5 °C to 8 °C (Broecker, 1991) Figure 23 shows production areas of deep overflow water. As seen by core JM11-FI-15GC the production of deep overflow water from has been fluctuating (Figure 10 and Figure 15) (see discussion above).

7.3 Heinrich event 4

H4 is the only Heinrich event seen in the investigated interval (Figure 18). This event is more extreme relative to other stadials. Not only does it have much larger changes in values, but it also has a longer duration. In core JM11-FI-15GC it spans from 40,628 – 39,151 cal. years BP, or approximately ~ 1500 years. In the data from Cortijo et al. (1997) they estimate that its duration was 1000 – 2000 years with temperature decrease of 2 °C. Roche et al. (2004) suggest that the duration of H4 was much shorter and rather 250 ± 150 years of duration and that the ice released in the event was

equivalent to a 2 ± 1 m in sea level rise. They used a climate model to simulate Heinrich event 4, using the distribution of oxygen isotopes in the oceans.

The data from JM11-FI-15GC is of very high resolution and if there was a small stadial before H4 it would most likely show in the data. There are some oscillations in the H4 interval, but no more than before or within other stadials, or in general in the $\delta^{18}O$ values (Figure 10). If there were a small stadial then there would also have to be a small warming positioned approximately around 40,194 – 40,021 cal. years BP (or at 284 – 282 cm). It would only span 173 years with an error of ± 449 years. The $\delta^{18}O$ value increases by 0.10 ‰, however that is not much more than the error of the mass spectrometer that was used, which is ± 0.06 ‰ for $\delta^{18}O$. This 'small warming' did not have an effect on bottom currents as magnetic susceptibility was decreasing. However, during this 'warming' there is decrease in ice rafted material (decrease by 295 IRD/g). Also, there is increase in % fragmentation, by 5.97 %, and decrease in concentration of foraminifera (488,78 foraminifera/g). If there was a small warming then it only affects the surface layer, not the bottom waters (Figure 10, 14 and 15). The warmer planktonic foraminifera would be helpful to estimate surface water changes, but as discussed before, their values are highly affected by changes in preservation and therefore not reliable for detailed interpretations. Even though the foraminifera are well preserved in this interval, there is increase in % fragmentation and decrease in concentration of foraminifera (Figure 19). Thus, there might be a small warming. However, even if the data is of high-resolution it is hard to interpret with confidence if there is a warming or if it just random fluctuations in the data.

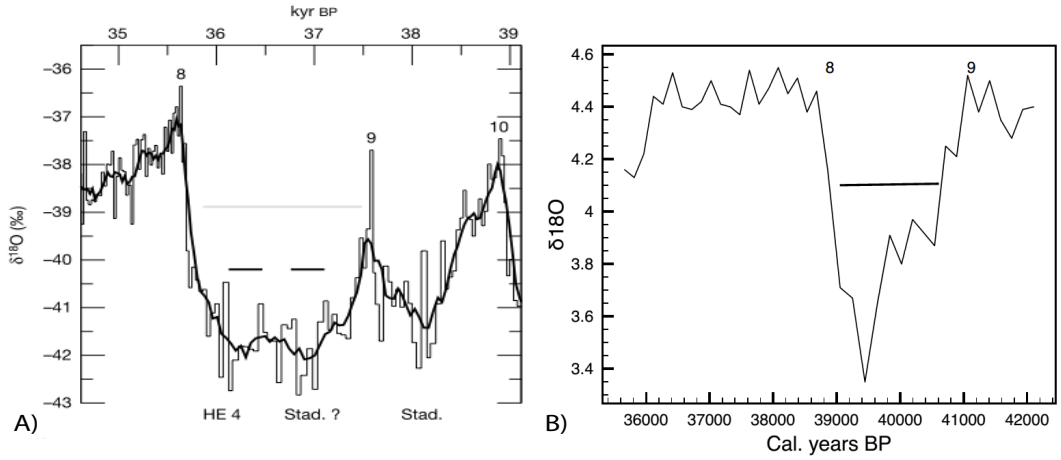

Figure 24(a) δ^{180} data is from Grip ice-core and it indicates a stadial interval before the Heinrich event 4 according to Roche et al. (2004). This indicates a very rapid climate change. The gray line in the figure from (Roche et al., 2004) shows the classical time used for Heinrich event 4, however the shorter black lines represents what they indicate as H4 and H4a stadial. Figure 22 (b) shows the data from core JM11-FI-15GC, the black line represents approximate interval of Heinrich event 4.

There are two types of Heinrich events seen within the Ruddiman belt, typical and atypical events. H4 is considered as a typical Heinrich event, as it receives most of the IRD from the Laurentide Ice sheet. But H4 also includes IRD originating from the Fennoscandian ice sheet. The Fennoscandian ice sheet collapsed along with the Laurentide ice sheet (Fronval et al., 1995). There is an indication that the European ice sheets released icebergs before the North American ice sheets (Snoeckx et al., 1999; Scourse et al, 2000). The data from JM11-FI-15GC would benefit from analyzing the type of IRD and their provenance, as is done in Rasmussen et al. (1998).

7.4 Tephra

Tephra layers come from explosive volcanic eruptions and have been found to be very beneficial for correlation purposes. These layers have been preserved in different environments such as on dry land, marine environments and within glaciers. Large volcanic eruptions can be used for fix-points, because they can be found spread over large areas, which is helpful when comparing records from different archives on land and in sea. It is also possible to geochemically analyze these layers and find out their origin with large certainties (Davies et al., 2010). Tephra layers are also useful for finding leads and lags, as airborne tephra might settle earlier on glaciers than at the bottom of the ocean (Wastegård et al., 2006). Greater understanding of leads and lags

can help us to develop better understanding of the paleoceanographic and climatic systems in the past (Rasmussen et al., 2003).

Faeroe Islands are a good place for studying tephra layers, as the islands are close enough to Iceland to receive the airborne tephra (Wastegård et al., 2006). Most of the porous tephra is carried by westerly winds to the islands from Iceland. The heavier particles, which are too heavy for the wind, can be transported by the bottom currents (Rasmussen et al., 2003). It is important to keep in mind that tephra particles often do not settle at the same time in different environments and can be reworked, as Griggs et al. (2014) have investigated in great detail.

7.4.1 The Faeroe Marine Ash Zones

The Faeroe Marine Ash Zones or FMAZ have been found to be very important for correlation purposes, because they have high synchronization with tephra found in the Greenland ice-core records (Griggs et al., 2014). The FMAZ-III is of special interest, because it is found within the investigated section of the core for this thesis and therefore special attention is given to that. FMAZ-III is both found in the Greenland ice cores and in marine cores from the Faeroe Islands (Wastegård et al., 2006, Rasmussen et al., 2003). This tephra layer is found close to the GI8 and it is thought that the fallout occurred around 100 years after the warming started for GI8 (Davies et al., 2010). The layers is also just above the H4, and it has been dated to approximately 33 ^{14}C ka BP, which makes it ideal for correlation (Rasmussen et al., 2003). However the NGRIP ice core gives an age of 38,122 ± 723 before 2000 years (Davies et al., 2010) and within core JM11-FI-15GC is falls around 38,760 ±432 cal. years BP. There is not a large difference between the ages, indicating that the marine reservoir effect may have been close to modern values. This supports the other evidence for ocean circulation and convection being close to modern conditions. In total fourteen tephra layers have been identified in the NGRIP record, in connection to FMAZ-III. The tephra spreads ~30 cm in core JM11-FI-15GC, which corresponds to almost 2000 years. Even though it is distributed over this large interval it still has two very large and sharp peaks (Figure 16) (Bourne et al., 2013).

The main complication with tephra layers in the marine realm is that it can be affected by secondary transport and depositional processes (Griggs et al., 2014). The small age difference between the ice-core and the gravity core indicate that the tephra

settled fast. It is doubtful that the tephra layer was disturbed much by bioturbation, as there was no indication of any activity when the core was examined. As indicated by (Griggs et al., 2014) it is unlikely that these two peaks (Figure 16) were caused by ice-rafting, as there is little of ice rafted material in this interval. The same result was seen in IRD values in core JM11-FI-15GC. It is suggested by Griggs et al. (2014) that the primary process working on the depositional signal was air fall.

FMAZ-III is of Icelandic origin, and is most likely comes from the Grímsvötn system. Bourne et al. (2013) argue though that this tephra layer is not that suitable for correlation as these are most likely series of closely timed eruptions that can only be separated in the high resolution ice-core records. Griggs et al. (2014) also suggested that it should only be used as isochron in high-resolution studies, where the individual tephras can be determined. This might not be very precise tie point to the Greenlandic ice sheet, however it serves as an indicator of the start of GI8

8 Conclusions

Due to the geographical position of the gravity core, JM11-FI-15GC, it is ideal for an investigation of water exchange between the Atlantic Ocean and the Nordic Seas in the past. In the investigated interval (42,189 – 33,393 cal. years BP) a total of four Dansgaard-Oeschger climatic events were identified, the largest cycle was used as a template for smaller events in this thesis. These Dansgaard-Oeschger events were divided into three intervals as seen in Rasmussen et al. (1996b). These three intervals are interstadials, transitional cooling intervals and stadials. The largest stadial interval found corresponded to Heinrich event 4.

The interstadial intervals have an abrupt beginning towards higher levels of magnetic susceptibility. There was also an increase in stable isotope values. This interval was characterized by strong bottom currents, with similar formation of North Atlantic deep water as today, as seen by the abundance of the benthic foraminiferal species *M. barleeanus.*

Decreasing bottom currents strength with increasing iceberg activity correlates with the transitional cooling intervals. These intervals seem to be less stable, as indicated by the high relative abundance of *E. excavatum*, which can tolerate environments, which might not be suitable for other foraminifera.

The formation of NADW stops or is greatly reduced during the stadials, due to the large influx of fresh water cause by increased iceberg activity, as seen by decreased values of $\delta^{18}O$. There is an indication of stratification by decreased values of $\delta^{13}C$. There is indication of Atlantic intermediate water at the bottom during the stadials as seen by occurrence of *C. neoteretis* and *C. reniforme*. Foraminiferal concentration is much higher in the stadials, due to better preservation. The ratio between planktonic and benthic foraminifera is also much higher. The foraminifera were best preserved in the stadials possibly due to low productivity. Stronger dissolution during the other intervals might have had strong implication on the data of distribution of planktic foraminiferal species. Therefore it was very important to count the fragments in every sample. If it had not been for fragmentation counting the increased indication of warm planktonic foraminifera of stadials would have led to wrong interpretation of the data.

References

Alley, R. B. and D. R. MacAyeal (1994). Ice-rafted debris associated with binge/purge oscillations of the Laurentide Ice Sheet. *Paleoceonography, 9*(4), 503-511.

Alve, E. and J. W. Murray (1999). Marginal marine environments of the Skagerrak and Kattegat: a baseline study of living (stained) benthic foraminiferal ecology. *Palaeogeography, Palaeoclimatology, Palaeoecology, 146,* 171-193.

Andersen, K. K., N. Azuma, J.-M. Barnola, M. Bigler, P. Biscaye, N. Caillon, J. Chappellaz, H. B. Clausen, D. Dahl-Jensen, H. Fishcer, J. Flückiger, D. Fritzsche, Y. Fujii, K. Goto-Azuma, K. Grønvold, N. S. Gundestrup, M. Hansson, C. Huber, C. S. Hvidberg, S. J. Johnsen, U. Jonsell, J. Jouzel, S. Kipfstuhl, A. Landais, M. Leuenberger, R. Lorrain, V. Masson-Delmotte, H. Miller, H. Motoyama, H. Narita, T. Popp, S. O. Rasmussen, D. Raynaud, R. Rothlisberger, U. Ruth, D. Samyn, J. Schwander, H. Shoji, M–L. Siggard-Andersen, J. P. Stefensen, T. Stocker, A. E. Sveinbjörnsdóttir, A. Svensson, M. Takata, J–L. Tison, Th. Thorsteinsson, O. Watanabe, F. Wilhelms and J. W. C. White (2004). High-resolution record of Northern Hemisphere climate extending into the last interglacial period. *Nature, 431,* 147-151.

Anderson, L. G., E. Flack, E. P. Jones, S. Jutterström and J. H. Swift (2004). Enhanced uptake of atmospheric CO_2 during freezing of seawater: A field study in Storfjorden, Svalbard. *Journal of geophysical research, 109,* 1-8.

Andrews, J. T. (2000). Icebergs and iceberg rafted detritus (IRD) in the North Atlantic: facts and assumptions. *Oceanography, 13*(3), 100-108.

Armstrong, H. A and M. D. Brasier (2009). *Microfossils.* Oxford: Blackwell publishing.

Bard, E (1988). Correction of accelerator mass spectrometry ^{14}C Ages measured in planktonic foraminifera: Paleoceanographic implications. *Paleoceanography, 3*(6), 635-645.

Bauch, D., J. Carstens and G. Wefer (1997). Oxygen isotope composition of living *Neogloboquadrina pachyderma* (sin.) in the Arctic Ocean. *Earth and Planetary Science Letters, 146*, 47-58.

Berger, W. H. (1971). Sedimentation of planktonic foraminifera. *Marine Geology, 11*(5), 325-358.

Bé, A. W. H. and D. S. Tolderlund (1971). Distribution and ecology of living planktonic foraminifera in surface water of the Atlantic and Indian Oceans. In B. M. Funnel and W. R. Riedel (Eds.), *The Micropaleontology of Oceans* (105-149). Cambridge: Cambridge University Press.

Blindheim, J. (1990). Arctic Intermediate Water in the Norwegian Sea. *Deep-Sea Research, 37*(9), 1475-1489.

Bond, G. C. and R. Lotti (1995). Iceberg Discharges into the North Atlantic on Millennial Time Scales During the Last Glaciation. *Science, 267*, 1005-1010.

Bond, G. C., W. Showers, M. Cheseby, R. Lotti, P. Almasi, P. deMenocal, P. Priore, H. Cullen, I. Hajdas and G. Bonandi (1997). A Pervasive Millennial-Scale Cycle in North Atlantic Holocene and Glacial Climates. *Science, 278,* 1257-1266.

Bond, G. C., W. Showers, M. Elliot, M. Evans, R. Lotti, I. Hajdas, G. Bonani and S. Johnson (1999). The North Atlantic's 1-2 kyr Climate Rhythm: Relation to Heinrich Events, Dansgaard/Oeschger Cycles and the Little Ice Age. *Mechanisms of Global Climate Change at Millennial Time Scales, 112,* 35-58.

Bond, G., H. Heinrich, W. Broecker, L. Labeyrie, J. McManus, Johan Andrews, S. Huon, R. Jantschik, S. Clasen, C. Simet, K. Tedesco, M. Klas, G. Bonani and S. Ivy (1992). Evidence for massive discharges of icebergs into the North Atlantic ocean during the last glacial period. *Nature, 360*, 245-249.

Bond, G., W. Broecker, S. Johnsen, J. McManus, L. Labeyrie, J. Jouzel and G. Bonani (1993). Correlations between climate records from North Atlantic sediments and Greenland ice. *Nature, 365*, 143-147.

Borenäs, K. and P. Lundberg (2004). Faroe-Bank Channel deep-water overflow. *Deep-Sea Research II, 51*, 335-350.

Bourne, A. J., S. M. Davies, P. M. Abbott, S. O. Rasmussen, J. P. Steffensen and A. Svenson (2013). Revisiting the Faroe Marine Ash Zone III in two Greenland ice cores: implications for marine-ice correlations. *Journal of Quaternary Science, 28*(7), 641-646.

Broecker, W. S. (1991). The Great Ocean Conveyor. *Oceanography, 4*(2), 1991.

Broecker, W. S., G. Bond and M. Klas (1990). A salt oscillator in the glacial Atlantic? 1. The concept. *Paleocenaography, 5*(4), 469-477.

Broecker, W., G. Bond, M. Klas, E. Clark and J. McManus (1992). Origin of the northern Atlantic's Heinrich events. *Climate Dynamics, 6*, 265-273.

Caralp, M. H. (1989). Size and morphology of the benthic foraminifer *Melonis barleeanum*: Relationships with marine organic matter. *Journal of Foraminiferal Research, 19*(3), 235-245.

Cayre, O., Y. Lancelot and E. Vincent (1999). Paleoceanographic reconstructions from planktonic foraminifera off the Iberian Margin: Temperature, salinity, and Heinrich events. *Paleoceanography, 14*(3), 384-396.

Clark, P. U, R. B. Alley and D. Pollard (1999). Northern Hemisphere Ice-Sheet Inlfluences on Global Climate Change. *Science, 286*, 1104-1111.

Cortijo, E., L. Labeyrie, L. Vidal, M. Vautravers, M. Chapman, J-C. Duplessy, M. Ellior, M. Arnold, J-L. Turon and G. Auffret (1997). Changes in sea surface hydrology associated with Heinrich event 4 in the North Atlantic Ocean between 40°and 60°N. *Earth and Planetary Science Letters, 146*, 29-45.

Dansgaard, W., S. J. Johnsen, H. B. Clausen, D. Dahl-Jensen, N. S. Gundestrup, C. U. Hammer, C. S. Hvidberg, J. P. Steffensen, A. E. Sveinbjörnsdóttir, J. Jouzel and G. Bond (1993). Evidence for general instability of past climate from a 250-kyr ice-core record. *Nature, 365*, 218-220.

Darling, K. F., K. D. Kroon and C. M. Wade (2006). A resolution for the coiling direction paradox in *Neogloboquadrina pachyderma*. *Paleoceanography, 21*, 1-14.

Davies, S. M., S. Wastegård, P. M. Abbott, C. Barbanate, M. Bigler, S. J. Johnsen, T. L. Rasmussen, J. P. Steffensen and A. Svensson (2010). Tracing volcanic events in the NGRIP ice-core and synchronising North Atlantic marine records during the last glacial period. *Earth and Planetary Science Letters, 294,* 69-79.

Dokken T. M. and E. Jansen (1999). Rapid changes in the mechanism of ocean convection during the last glacial period. *Nature, 40*, 458-461.

Ernst, S., R. Bours, I. Duijnstee and B. van der Zwaan (2005). Experimental effects of an organic matter pulse and oxygen depletion on a benthic foraminiferal shelf community. *Journal of Foraminiferal Research, 35*(3), 177-197.

Ezat, M. M., T. L. Rasmussen and J. Groeneveld (2014). Persistent intermediate water warming during cold stadils in the southeastern Nordic seas during the past 65. k.y.. *Geology, 42*(8), 663-666.

Fairbanks, R. G., R. A. Mortlock, T-C. Chiu, L. Cao, A. Kaplan, T. P. Guilderson, T. W. Fairbanks, A. L. Bloom, P. M. Grootes and M-J. Nadeau (2005). Radiocarbon

calibration curve spanning 0 to 50,000 years BP based on paired $^{230}Th/^{234}U/^{238}U$ and ^{14}C dates on pristine corals. *Quaternary Science Reviews*, *24,* 1781-1796.

Feyling-Hanssen, R. W. (1972). The foraminifer *Elphidium excavatum* (Terquem) and its variant forms. *Micropaleontology*, *18*(3), 337-354.

Fronval, T., E. Jansen, J. Bloemendal and S. Johnsen (1995). Oceanic evidence for coherent flucuations in Fennoscandian and Laurentide ice sheets on millennium timescales. *Nature, 374,* 443-446.

Geotek (2014). Multi-Sensor Core Logger [Manual]. Northhamtonshire: Geotek Ltd.

Gordon, A. L. (1986). Interocean Exchange of Thermocline Water. *Geophysical Research, 91*(C4), 5037-5046.

Griggs, A. J., S. M. Davies, P. M. Abbott, T. L. Rasmussen and A. P. Palmer (2014). Optimising the use of marine tephrochronology in the North Atlantic: a detialed investigation of the Faroe Marine Ash Zone II, III, and IV. *Quaternary Science Reviews, 106*, 122-139.

Grousset, F. E., L. Labeyrie, J. A. Sinko, M. Cremer, G. Bond, J. Duprat, E. Cortijo and S. Huon (1993). Patterns of ice-rafted detritus in the glacial north Atlantic (40-55°N). *Paleoceanography, 8*(2), 175-192.

Gustafsson, M. and K. Nordberg (2001). Living (Stained) benthic foraminiferal response to primary production and hydrography in the deepest part of the Gullmar fjord, Swedish west coast, with comparisons to Höglund's 1927 material. *Journal of Foraminiferal Research, 31*(1), 2-11.

Hald, M. and P. I. Steinsund (1996). Benthic foraminifera and carbonate dissolution in the surface sediments of the Barents and Kara seas. *Reports on Polar research, 212,*285-307.

Hald, M. and S. Korsun (1997). Distribution of modern benthic foraminifera from fjords of Svalbard, european arctic. *Journal of Foraminiferal Research, 27*(2), 101-122.

Hansen, A. and K. L. Knudsen (1995). Recent foraminiferal distribution in Freemansundet and Early Holocene stratigraphy on Edgeøya, Svalbard. *Polar Research, 14*(2), 215-238.

Hansen, B. and S. Østerhus (2000). North Atlantic-Nordic Seas exchanges. *Progress in Oceanography, 45*, 109-208.

Hansen, B., S. Østerhus, W. R. Turrell, S. Jónsson, H. Valdimarsson, H. Hátún and S. M. Olsen (2008). The Inflow of Atlantic Water, Heat, and Salt to the Nordic Seas Across the Greenland-Scotland Ridge. Dickson, R.R, J. Meincke and P. Rhines (Eds.). *Arctic-Subarctic Ocean Fluxes* (15-43). Netherlands: Springer.

Hays, J. D., J. Imbrie and N. J. Shackleton (1976). Variations in the Earth's Orbit: Pacemaker of the Ice Ages. *Science, 194,* 1121-1132.

Hebbeln, D., R. Henrich and K-H. Baumann (1998). Paleoceanography of the last interglacial/glacial cycle in the polar north Atlantic. *Quaternary Science Reviews, 17*, 125-153.

Heinrich, H. (1988). Origin and Consequences of Cyclic Ice rafting in the Northeast Atlantic Ocean during the Past 130,000 Years. *Quaternary Research, 29,* 142-152.

Hemming, S. R. (2004). Heinrich events: Massive late pleistocene detritus layers of the north Atlantic and their global climate imprint. *Review of Geophysics, 42*, 1-43.

Hohbein, M. W., P. F. Sexton and J. A. Cartwright (2012). Onset of North Atlantic Deep Water production coincident with inception of the Cenozoic global cooling trend. *Geology, 40*(3), 255-258.

Hulbe, C. L. (1997). An ice shelf mechanism for Heinrich layer production. *Paleoceanography, 12*(5), 711-717.

Hulbe, C. L., D. R. MacAyeal, G. H. Denton, J. Kleman and T. Lowell (2004). Catastrophic ice shelf breakup as the source of Heinrich event icebergs. *Paleoceanography, 19,* 1-15.

Hunt, A. S. and B. H. Corliss (1993). Distribution and microhabitats of living (stained) benthic foraminifera from the Canadian Arctic Archipelago. *Marine Micropaleontology, 20,* 321-345.

Jennings, A. E. and G. Helgadóttir (1994). Foraminiferal assemblages from the fjords and shelfs of Eastern Greenland. *Foraminiferal Research, 24*(2), 123-144.

Jennings, A. E., N. J. Weiner, G. Helgadóttir and J. T. Andrews (2004). Foraminiferal faunas of the Southern to Northern Iceland shelf: Oceanographic and environmental controls. *Journal of Foraminiferal Research, 34*(3), 180-207.

Johnsen, S. J., D. Dahl-Jensen, N. Gundestrup, J. P. Steffensen, H. B. Cluasen, H. Miller, V. Masson-Delmotte, A. E. Sveinbjörnsdóttir and J. White (2001). Oxygen isotope and palaeotemperature records from six Greenland ice-core

stations: Camp Centuary, Dye-3, GRIP, GISP2, Renland and NorthGRIP. *Journal of Quaternary Science, 16*(4), 299-307.

Johnsen, S. J., H. B. Clausen, W. Dansgaard, K. Fuhrer, N. Gundestrup, C. U. Hammer, P. Iversen, J. Jouzel, B Stauffer and J. P. Steffensen (1992). Irregular glacial interstadials recorded in a new Greenland ice core. *Nature, 359*, 311-313.

Johnson, R. G. and S–E. Lauritzen (1995). Hudson Bay-Hudson Strait jökulhlaups and Heinrich events: a hypothesis. *Palaeogeoprahy, Palaecoclimatology, Palaeoevology, 117,* 123-137.

Kellogg, T. B. (1980). Paleoclimatology and paleo-oceanography of the Norwegian and Greenland seas: glacial-interglacial contrasts. *Boreas, 9*, 115-137.

Kissel. C., C. Laj, L. Labeyrie, T. Dokken, A. Voelker and D. Blamart (1999). Rapid climatic variations during marine isotopic stage 3: magnetic analysis of sediments from Nordic Seas and North Atlantic. *Earth and Planetary Science Letters, 171,* 489-502.

Kroopnick, P. M. (1985). The distribution of ^{13}C of ΣCO_2 in the world oceans. *Deep-Sea Research, 32*(1), 57-84.

Le, J. and N. J. Shackleton (1992). Carbonate dissolution fluctuations in the westren equatorial Pacific during the late quaternary. *Paleoceanography, 7*(1), 21-42.

Linke, P. and G. F. Lutze (1993). Microhaibitat preferences of benthic foraminifera- a static concept or a dynamic adaptation to optimize food acquistion? *Marine Mircropaleontology, 20*, 215-234.

Linsley, B. K. and R. B. Dunbar (1994). The late Pleistocene history of surface water $\delta^{13}C$ in the Sulu Sea: Possible relationship to Pacific deepwater $\delta^{13}C$ changes. *Paleoceanography, 9*(2), 317-340.

MacAyeal, D. R. (1993). Binge/purge oscillations of the Laurentide ice sheet as a cause of the north Atlantic's Heinrich events. *Paleoceanograpy, 8*(6), 775-784.

MacKensen, A. and M. Hald (1988). *Cassidulina teretis* Tappan and *C. leavigata* D'orbigny: Modern and late Quaternary distribution in Northern seas. *Journal of Foraminiferal Research, 18*(1), 16-24.

Marcott, S. A., P. U. Clark, L. Padman, G. P. Klinkhammer, S. R. Springer, Z. Liu, B. L. Otto-Bliesner, A. E. Carlson, A. Ungerer, J. Padman and F. He (2011). Ice-shelf collapse from subsurface warming as a trigger for Heinrich events. *PNAS, 108*(33), 13,415-13,419.

Maslin, M. A., N. J. Shackleton and U. Pflaumann (1995). Surface water temperature, salinity and density changes in the northeast Atlantic during the last 45,000 years: Heinrich events, deep water formation, and climatic rebounds. *Paleoceanography, 10*(3), 527-544.

Maslin, M., D. Seidov and J. Lowe (2001). Synthesis of the Nature and Causes of Rapid Climate Transitions During the Quaternary. D. Seidov, B. J. Haupt and M. maslin (eds). *The Oceans and Rapid Climate Change: Past, Present and Future.* (9-52). Washington: American Geophysical Union.

McManus, J. F., R. Francols, J-M. Gherardi, L. D. Keigwin and S. Brown-Leger (2004). Collapse and rapid resumption of Atlantic meridional circulation linked to deglacial climate changes. *Nature, 428,* 834-837.

Meincke, J. (1977). On the distribution of low salinity intermediate water around the Faroes. *Deutsche Hydrographische Zeitschrift, 31,* 50-64.

Mix, A. C. and W. F. Ruddiman (1982). Oxygen-Isotope Analyses and Pleistocene Ice Volumes. *Quaternary research, 21*, 1-20.

Moros, M., A. Kuijpers, I. Snowball, S. Lassen, D. Bäckström, F. Gingele and J. McManus (2002). Were glacial iceberg surges in the North Atlantic triggered by climatic warming? *Marine Geology, 192,* 393-417.

Mudie, P. J., C. E. Keen, I. A. Hardy and G. Vilks (1984). Multivariate analysis and quantitative paleoecology of benthic foraminifera in surface and late quaternary shelf sediments, Northern Canada. *Marine Micropaleontology, 8,* 283-313.

Olsen, J. T. L. Rasmussen and P. J. Reimer (2014). North Atlantic marine radiocarbon reservoir ages through Heinrich event H4: a new method for marine age model construction. *Geological Society, London, Special Publication, 398,*95-112.

Orvik K. A. and P. Niiler (2002). Major pathways of Atlantic water in the northern North Atlantic and Nordic Seas toward Arctic. *Geophyscial Research Letters, 29*(19), (1 – 4).

Paterne, M., N. Kallel, L. Labeyrie, M. Vautravers, J-C. Duplessy, M. Rossignol-Strick, E. Cortijo, M. Arnold and M. Fontugne (1999). Hydrological relationship between the North Atlantic Ocean and the Mediterranean Sea during the past 15 – 75 kyr. *Paleoceanography, 14*(5), 626-638.

Peck, V. L., I. R. Hall, R. Zahn and J. D. Scourse (2007). Progressive reduction in NE Atlantic intermediate water ventilation prior to Heinrich events: Response to NW European ice sheet instabilities? *Geochemistry, Geophysics, Geosystems, 8*(1), 1-11.

Pisias, N. G. and T. C. Moore, Jr (1981). The evolution of Pleistocene climate: a time series approach. *Earth and Planetary Science Letters, 52*, 450-458.

Polyak, L., S. Korsun, L. A. Febo, V. Stanovoy, T. Khusid, M. Hald, B. E. Paulsen and D. J. Lubinski (2002). Benthic foraminiferal assemblages from the southern Kara sea, a river-influenced arctic marine envrionment. *Journal of Foraminiferal Research, 32*(3), 252-273.

Ramussen, T. L., D. Bäckström, J. Heinemeier, D. Klitgaard-Kristensen, P. C. Knutz, A. Kuijpers. S. Lassen, E. Thomsen, S. R. Troelstra and T. C. E. van Weering (2002b). The Faroe-Shetland Gateway: Late Quaternary water mass exchange between the Nordic seas and the northeastren Atlantic. *Marine Geology, 188,* 165-192.

Rasmussen, T. L. and E. Thomsen (2004). The role of the North Atlantic Drift in the millennial timescale glacial climate fluctuations. *Palaeogeography, Palaeoclimatology, Palaeoecology, 210,* 101-116.

Rasmussen, T. L. and E. Thomsen (2014). Brine formation in relation to climate changes and ice retreat during the last 15,000 years in Storfjorden, Svalbard, 76-78°N. *Paleoceanography, 29,* 911-929.

Rasmussen, T. L. and T. Nielsen (2011). *Cruise report, marine-geological cruise to the Faroe Islands, R/V Jan Mayen, April 26th-May 11th 2011*. Tromsø: University of Tromsø, Department of Geology.

Rasmussen, T. L., E. Thomsen and T. C. E. van Weering (1998). Cyclic sedimentation on the Faeroe Drift 53-10 ka BP related to climatic variations. *Geological Society Special Publication 1998, 129*, 255-267.

Rasmussen, T. L., E. Thomsen, L. Labeyrie and T. C. E. van Weering (1996a). Circulation changes in the Faeroe-Shetland Channel correlating with cold events during the last glacial period (58-10 ka). *Geology, 24*(10), 937-940.

Rasmussen, T. L., E. Thomsen, S. R. Troelstra, A. Kuijpers and M. A. Prins (2002a). Millennial-scale glacial variability versus Holocene stability: changes in planktic and benthic foraminifera faunas and ocean circulation in the North Atlantic during the last 60 000 years. *Marine Mircropaleontology, 47*, 143-176.

Rasmussen, T. L., E. Thomsen, T. C. E. van Weering and L. Labeyrie (1996b). Rapid changes in surface a nd deep water conditions at the Faeroe Margin during the last 58,000 years. *Paleoceanograpy, 11*(6), 757-771.

Rasmussen, T. L., S. Wastegård, A. Kuijpers, T. C. E. van Weering, J. Heinemeier and E. Thomsen (2003). Stratigraphy and distribution of tephra layers in marine sediment cores from the Faeroe Islands, North Atlantic. *Marine Geology, 199,* 263-277.

Rhamstorf, S. (2003). Timing of abrupt climate change: A precie clock. *Geophysical Research Letters, 30*(10), 1-4.

Robinson, S. G., M. A. Maslin and I. N. McCave (1995). Magnetic susceptibility variations in Upper Pleistocene deep-sea sediments of the NE Atlantic: Implications for ice rafting and paleocirculation at the last maximum. *Paleoceanography, 10*(2), 221-250.

Roche, D., D. Paillard and E. Cortijo (2004). Constraints on the duration and freshwater release of Heinrich event 4 through isotope modelling. *Nature, 432*, 379-382.

Ruddiman, W. F. (1977). Late Quaternary deposition of ice-rafted sand in the subpolar North Atlantic (lat 40°to 65°N). *Geological Society of America Bulletin, 88,* 1813-1827.

Ruddiman, W. F., M. Raymo and A. McIntyre (1986). Matuyama 41,000 cycles: North Atlantic Ocean and northern hemisphere ice sheets. *Earth and Planetary Science Letters, 80*, 177-129.

Sánchez Goñi, M. F., J-L. Turon, F. Eynaud and S. Gendreau (2000). European Climatic Response to Millennial-Scale Changes in the Atmosphere-Ocean System during the Last Glacial Period. *Quaternary Research 54,* 394-403.

Schafer C. T. and F. E. Cole (1982). Living benthic foraminifera distributions on the continetal slope and rise east of Newfoundland, Canada. *Geological Society of America Bulletin, 93*, 207-217.

Schmidt, D. N., S. Renaud, J. Bollmann, R. Schiebel and H. R. Thierstein (2004). Size distribution of Holocene planktic foraminifer assemblages: biogeography, ecology and adaptation. *Marine Micropaleontology, 50*, 319-338.

Scott, D. B., P. J. Mudie, G. Vilks and D. C. Younger (1984). Late Pleistocene-Holocene paleoceanographic trends on the continental margin of eastern Canada:

Foraminiferal, dinoflagellate and pollen evidence. *Marine Micropaleontology, 9*, 181-218.

Scott, D. B., T. Schell, A. Rochon and S. Blasco (2008). Modern benthic foraminifera in the surface sediments of the Beaufort shelf, slope and Mackenzie through, Beaufort sea, Canada: Taxonomy and summary of surfical distributions. *Journal of Foraminiferal Research, 38*(3), 228-250.

Scourse, J. D., I. R. Hall, I. N. McCave, J. R. Young and C. Sugdon (2000). Origin of Heinrich layers: evidence from H2 fro European precursor events. *Earth and Planetary Science Letters.*

Snoeckx, H., F. Grousset, M. Revel and A. Boelaert (1999). European contribution of ice-rafted sand to Heinrich layers H3 and H4. *Marine Geology, 158,* 197-208.

Steinsund, P. I. and M. Hald (1994). Recent calcium carbonate dissolution in the Barents Sea: Paleoceanographic applications. *Marine Geology*, *177,* 303-316.

Steinsund, P. I., L. Polyak, M. Hald, V. Mikhailov and S. Korsun (1994). Distribution of calcareous benthic foraminifera in recent sediments of the Barents and Kara Seas. *Unpublished*.

Svensson, A., K. K. Andersen, M. Bigler, H. B. Clausen, D. Dahl-Jensen, S. M. Davies, S. J. Johnsen, R. Muscheler, F. Parrenin, S. O. Rasmussen, R. Röthlisberger, I. Seierstad, J. P. Steffensen and B. M. Vinther (2008). A 60 000 year Greenland stratigraphic ice core chronology. *Climate of the Past, 4,* 47-57.

Sørensen, A. B. (2003). Cenozoic basin development and stratigraphy of the Faroes area. *Petroleum Geoscience, 9*(3), 189-207.

Turrell, W. R., G. Slesser, R. D. Adams, R. Payne and P. A. Gilliband (1999). Decadal variability in the composition of Faroe Shetland Channel bottom water. *Deep-Sea Research, 46*, 1-25.

Vidal, L., L. Labeyrie, E. Cortijo, M. Arnold, J. C. Duplessy, E. Michel, S. Becqué and T. C. E. van Weering (1997). Evidence for changes in the North Atlantic Deep water linked to meltwater surges during the Heinrich events. *Earth and Plantery Science Letters, 146*, 13-27.

Vilks, G. (1981). Late Glacial-Postglacial Foraminiferal Boundary in Sediments of Eastern Canada, Denmark and Norway. *Geoscience Canada, 8*(2), 48-55.

Wastegård, S., T. L. Rasmussen, A. Kuijpers, T. Nielsen and T. C. E. van Weering (2006). Composition and origin of ash zones from Marine Isotope Stages 3 and 2 in the North Atlantic. *Quaternary Science Reviews, 25*, 2409-2419.

Zamelcyzk, K., T. L. Rasumssen, K. Husum and M. Hald (2013). Marine calcium carbonate preservation vs. climate change over the last two millennia in the Fram Strait: Implications for planktic foraminiferal paleostudies. *Marine Micropaleontology, 98*, 14-27.

Zamelczyk, K, T. L. Rasmussen, K. Husum, H. Hafliðason, A. de Vernal, E. K. Ravna, M. Hald and C. Hillaire-Marcel (2012). Paleoceanographic changes and calcium carbonate dissolution in the central Fram Strait during the last 20 ka yr. *Quaternary Research, 78,* 405-416.

Appendix

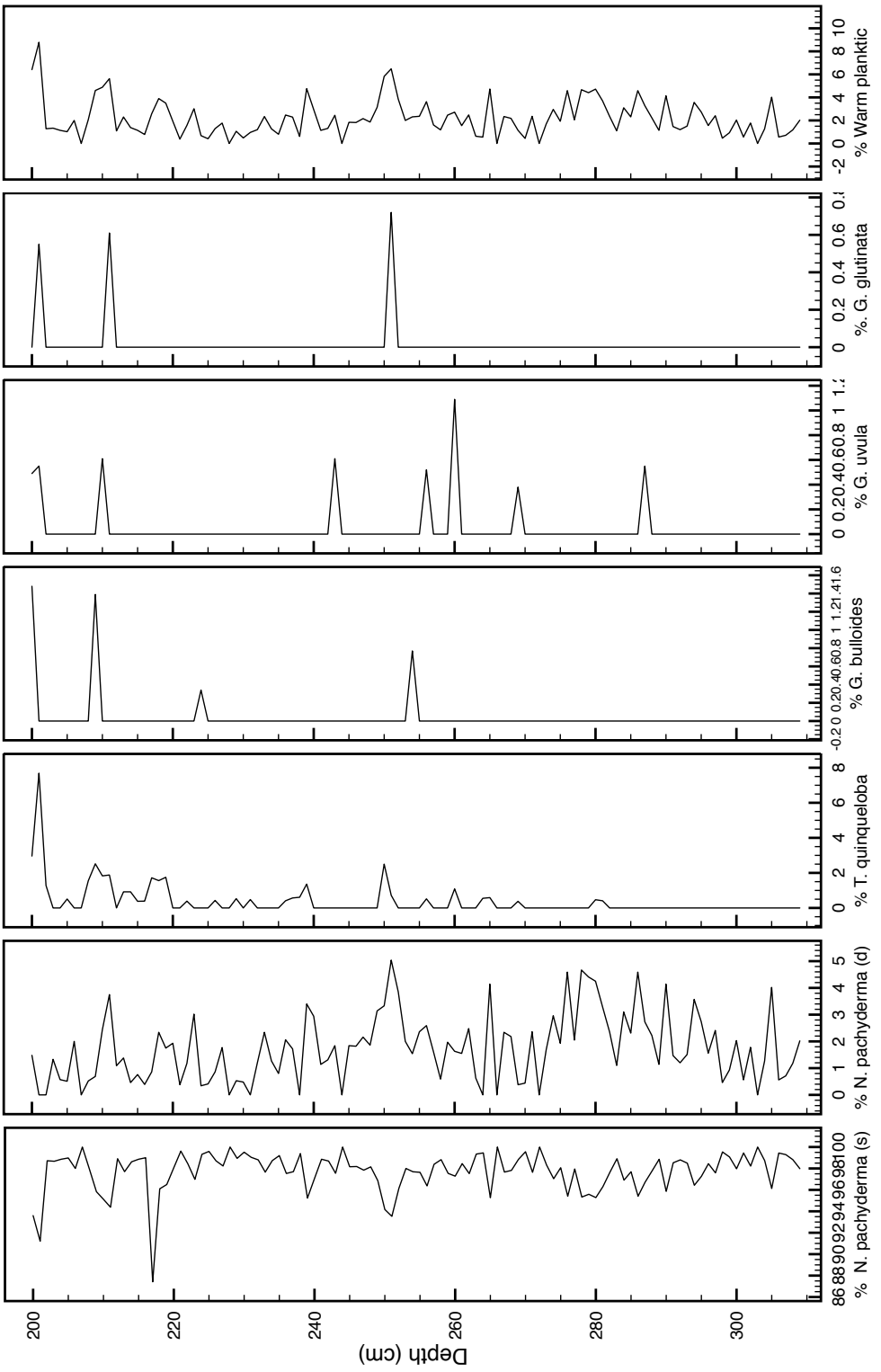

Figure 25 Planktonic foraminifera in core JM11-FI-15GC.